DISSERTATIONES
MATHEMATICAE
UNIVERSITATIS
TARTUENSIS
141

SHAHID MUBASSHAR

Natural vibrations of curved nanobeams

DISSERTATIONES MATHEMATICAE UNIVERSITATIS TARTUENSIS
141

DISSERTATIONES MATHEMATICAE UNIVERSITATIS TARTUENSIS
141

SHAHID MUBASSHAR

Natural vibrations of curved nanobeams

UNIVERSITY OF TARTU
Press
1632

Institute of Mathematics and Statistics, Faculty of Science and Technology, University of Tartu, Estonia.

Dissertation has been accepted for the commencement of the Degree of Doctor of Philosophy (PhD) in Mathematics on September 08, 2023 by the council of the Institute of Mathematics and Statistics, Faculty of Science and Technology, University of Tartu.

Supervisor: Professor Jaan Lellep, D. Sci.
Institute of Mathematics and Statistics
University of Tartu, Estonia

Opponents: Professor Rimantas Kačianauskas,
Member of Lithuanian Academy of Science
Department of Applied Mechanics
Vilnius Gediminas Technical University Vilnius, Lithuania

Professor János Lógó
Department of Structural Mechanics
Budapest University of Technology and Economics, Hungary

Commencement will take place on September 29, 2023 at 14:15 in Narva mnt 18-1020.

The publication of this dissertation is financed by the Tartu ASTRA Project PER ASPERA (European Regional Development Fund) and Institute of Mathematics and Statistics, University of Tartu.

ISSN 1024-4212 (print) ISSN 2806-240X (pdf)
ISBN 978-9916-27-329-6 (print) ISBN 978-9916-27-330-2 (pdf)

University of Tartu Press
http://www.tyk.ee

List of original publications

1. J. Lellep and S. Mubasshar, Nonlocal theory of elasticity in the natural vibrations of curved CNTs with defects, Proc. Conf. Indust. Appl. Math. (submitted).

2. J. Lellep and S. Mubasshar, Natural vibrations of circular nanoarches of piecewise constant thickness, Acta Comment. Math. Tartu (submitted).

3. J. Lellep and S. Mubasshar, Natural vibrations of nonlocal curved clamped nanobeams. J. Vib. Control (submitted).

4. J. Lellep and S. Mubasshar, Natural vibrations of curved nanobeams and nanoarches, Acta Comment. Math. Tartu 26 (2022), 63-76.

5. A. Majeed, A. Zeeshan, and S. Mubbashir. Vibration analysis of carbon nanotubes based on cylindrical shell by inducting Winkler and Pasternak foundations. Mech. Adv. Mater. Struct. 26(2019), 1140-45.

Contents

List of Figures

List of Tables

Nomenclature

α_i	position of the crack
β	central angle
Γ	arbitrary closed contour around the crack tip
∇^2	nabla operator
ν	Poisson ratio
ω	natural frequency of vibration
ρ	density of the material
σ_{ij}^c	stress tensor in classical elasticity
σ_{ij}	stress tensor for the nonlocal theory
ε	relative extension of the curved element
$\varkappa$	curvature of the middle line of the nanoarch
φ	current angle
a	dimension of the lattice of the material
b	width of the nanoarch
C	compliance
c_i	depth of the crack

d diameter of the CNTs

E Young's modulus

e_0 material constant

G energy release rate

h_i thickness of the nanoarch

I moment of inertia of a cross-sectional area of the nanoarch

M bending moment

N membrane force

p external loads in the radial direction

P_i generalised stress in the fracture mechanics

p_u external loads in transverse direction

Q shear force

R radius of the central line of the arch

t time

T_i external forces

U displacement in the circumferential direction

u_i generalised displacements

U_s strain energy density

W displacement in the transverse direction

Acronyms

S-S simply supported

C-C clamped-clamped

C-F clamped-free

C-S clamped-simply supported

CNT carbon nanotube

SWCNT single walled carbon nanotube

MWCNT multi walled carbon nanotube

MEMS microelectromechanical systems

NEMS nanoelectromechanical systems

Chapter 1

Introduction

1.1 Historical review of the literature and motivation

The arch, also known as a curved beam, supports and distributes loads along its curved shape [60]. As ones of the eldest structural elements [136], arches have been widely utilised in various industrial fields due to their ability to transfer loads through bending and stretching for in-plane deformations [14, 29, 77]. The study of arches can be traced back to the works of Hartog [36] and Love [94]. In modern times, it has encompassed extensive investigations covering practical applications and theoretical formulations [71, 101, 108, 139, 150]. During their application, arches are subjected to different mechanical stresses, such as tension, compression, and vibration, which must be effectively controlled beforehand. Numerous researchers have conducted extensive studies on these forces [14, 15, 78, 93, 96, 113]. By comprehensively examining the behaviour and responses of arches under various forces, valuable insights are gained to enhance their performance and ensure their reliable application.

Since the beginning of the current century, nanomaterials have gained significant usage in many structures due to their unique properties. The surface area to volume ratio increases in nanomaterials compared to

macro materials. This ratio contributes to making nanomaterials highly conductive and more reactive [1, 87, 88]. That is why curved nanobeams or arches play a significant role in the design and functionality of Microelectromechanical Systems (MEMS) and Nanoelectromechanical Systems (NEMS) [45, 109, 141]. However, it is essential to study the behaviour of nanoarches under external loading, especially in industrial applications. Vibration is an integral part of many structures. To avoid the adverse effects of vibrations, such as resonance, it is essential to calculate the natural frequency of nanoarches to mitigate the effects. Therefore, calculating the natural frequency of nanoarches is crucial before their incorporation into the structures. Researchers have widely adopted techniques such as molecular dynamics and numerical methods to study the nanostructures, which have been widely accepted due to their applicability and ease of use [2, 3, 98, 111].

However, the classical theory of elasticity cannot predict the small-length scale effects effectively. To tackle this limitation, Eringen [46] introduced the nonlocal theory of elasticity to study the dynamic behaviour of nanomaterials. Research on the dynamic behaviour of curved nanobeams using this novel approach has attracted popularity in recent decades and got acceptance by many scientists. Originally Eringen and Edelen [47] applied the nonlocal constitutive model to investigate surface waves and screw dislocations in solids. Later the nonlocal beam theory was used for the investigation of the bending problems by Reddy [115], Thai [135], Li and Wang [88], Li et al. [86], Reddy and Pang [116], Civalek und Demir [33] by making use of the Euler-Bernoulli beam model, also by Roque et al. [121], Wang, Zhang and He [145] in the case of the Timoshenko beam model.

Buckling and vibration of nanobeams were studied by many investigators, including Ansari and Sahmani [10], Roostai and Haghpanahi [120], Sahmani and Ansari [123], Behera and Chakraverty [21], Aydogdu [16], Thai [134, 135], Thai, Vo, Nguyen and Kim [135], Murmu and Pradhan [106], Wang, Zhang and He [145], Ganapathi and Polit [51], Bağdatli [18], Wang, Zhang, Ramesh and Kitipornchai [146], Wang, Zhang, Challamel and Duan [144], Wang and Arash [147] and others. Notably, Aydogdu [16] utilised the nonlocal constitutive equations

developed by Eringen [46] and used various beam theories, including Euler-Bernoulli, Timoshenko, and Reddy theories. Wang and Duan [141] applied the nonlocal theory of elasticity to calculate the natural frequency of circular nanorings. To validate the effects of the nonlocal theory, they compared the results with those obtained in classical theories. By employing the nonlocal theory of elasticity, researchers have explored and comprehensively understood the dynamic characteristics of nanomaterials in the form of curved nanobeams.

Applying the nonlocal theory of elasticity has expanded our understanding of the dynamic characteristics of nanomaterials. This comprehensive exploration has shed light on the intricate nature of these structures, contributing to advancements in the field. Zhang et al. [156] conducted a study where they calibrated the small length scale coefficient and observed its variation in response to changes in other physical parameters. Polit et al. [112] also investigated the influence of structural and material parameters on the buckling behaviour of curved nanobeams by solving Eringen's strain-driven integral model. Further investigation by Ebrahimi and Daman [41] focused on the nonlocal elasticity model to investigate the effects of various parameters, including those related to elastic foundations, on the natural vibration and critical buckling of the curved nanobeams.

More next papers [11, 40, 42, 51, 117] present works on nonlocal curved beams' bending, buckling, and vibration analysis. In another study, Zenkour and Radwan [155] utilised the nonlocal strain gradient theory to examine the effects of different boundary conditions and stresses on the vibrations of porous functionally graded curved nanobeams. Furthermore, Wang et al. [143] investigated the buckling behaviour of circular arches, focusing on the impact of small-length scale effects and the critical buckling pressure. The influence of the nonlocal parameter on the natural frequency of curved nanobeams has been demonstrated by Moosavi et al. [105], further establishing its significance. Moreover, several researchers have extended the application of the nonlocal theory of elasticity to investigate the dynamic behaviour of nanowires, nanoplates, and carbon nanotubes [39, 73, 106, 107, 127, 148, 154]. Examining mechanical properties, Wu and Yu [149] considered rectangular

nanobeams and single-walled and multi-walled carbon nanotubes. They formulated the relevant equations using the nonlocal beam theory of elasticity. On the other hand, Ebrahimi and Barati [40] focused on investigating the natural vibrations of curved nanobeams in thermal environments. Similarly, many scientists have utilised the nonlocal beam theory to analyse the specific effects of surface properties, temperature, and rotary inertia on the natural vibrations of nanobeams [12, 23, 43, 97, 126]. In a related study, Ke et al. [72] explored the concept of free vibrations of nonlocal beams under various factors, including electric potential, magnetic potential, and temperature. They discovered that these factors significantly influence the natural frequency of the beams. Furthermore, Simsek [128] exhibited the free vibration of nanobeams with large amplitudes, focusing specifically on the impact of the nonlocal parameter on the nonlinear frequency ratio.

Moreover, several researchers [7, 24, 25, 49, 52, 53, 55, 59, 65] incorporated fracture mechanics concepts in their books and papers. Maknickas et al. [99] studied the fracture risk of the mechanical system. Tretjakovas, Kačianauskas and Šimkevičius [138] presented deformation and rupture analysis of the shock tube diaphragm behaviour under pressure. Ahmadvand and Asadi [4], Chinka et al. [30], Kala [67], Kumar and Singh [76], Rosa and Lippiello [122], Sen and Khazanovich [125] explored the behaviour of cracks as newly generated surfaces that remain intact with their original structures. Cannizzaro et al. [26] presented a distributional approach to formulating the free vibration equations for circular arches with multiple cracks using Dirac's deltas. In their paper, closed-form solutions are obtained for the vibration modes and frequencies and compared with experimental and numerical results. The existence of cracks and other flaws within structural components introduces additional flexibility.

Several researchers have investigated the increased flexibility caused by the crack using elastic springs. Anifantis and Dimarogonas [8], Dimarogonas [38], Chondros et al. [31, 32], Rizos et al. [119], and Kukla [75] have investigated the task with the help of the increased flexibility caused by a crack using an elastic spring. They applied this approach to vibrating beams and bars where cracks had weakened them. Lellep

and Kägo [79] extended this methodology to elastic plate strips. Cracks can appear on the surfaces of the body due to various aspects such as environmental effects, wear and tear, inappropriate loading conditions, and operational conditions. Cracks also influence the natural frequency of the nanostructures, as shown by Eroglu and Tufekci [48] and Lellep and Mubasshar [84]. Mode shape also changes due to cracks, as shown by Hossain and Lellep [61], Song et al. [130], and Wu et al. [151]. Scientists have shown great interest in studying cracked nanobeams and nanoarches due to the presence of cracks in the nanomaterials and their influence on the natural frequency. In this regard, the application of nonlocal theory gained attention once more. Roostai and Haghpanahi [120] studied the effects of cracks on the natural frequency of nonlocal beams. Torabi and Dastgerdi [137] demonstrated that the crack location in the nonlocal beam also affects the natural frequency, along with other parameters such as rotary inertia and nonlocal parameter. Loya et al. [95] explored the discontinuity in the bending slope caused by cracks in the nanobeam.

In the published literature, one can find a limited number of papers concerning the vibration and stability of nanobeams, nanoplates and nanorings with cracks. Loghmani and Yazdi [92] develop an analytical method for determining natural frequencies of cracked nanobeams with stepped cross-sections. The case of a cantilever nanobeam with a buckyball at the free end is studied separately in [62]. Curved beams and segments of rings with cracks are the objects of investigations by Karaagac, Öztürk and Sabuncu [68, 69], also by Cerri and Ruta [28] and Cerri, Dilena and Ruta [27], also Krawczuk et al. [74]. Viola, Artioli, and Dilena [139] investigate in-plane free vibrations of circular arches with defects and Viola and Tornabene [140], Chondros et al. [31], also by Mazanoglu and Sabuncu [103] and Mazanoglu et al. [102]. Hashemi et al. [57] illustrated that the surface effects on the natural frequency depend on the length of the nanobeam.

Furthermore, Hsu [64] showed that increasing the nonlocal parameter reduces the impact of damages on the nanobeams' natural frequency. In subsequent studies, Hasheminejad et al. [58], Aria et al. [13], and Baharami [19] also investigated the effects of cracks and other param-

eters on the natural frequency of the nanobeams. In [19], it was found that the natural frequency decreases with an increase in the nonlocal parameter. However, in the case of a cantilever nanobeam, the natural frequency increases with the rise in the nonlocal parameter. These studies collectively contribute to our understanding of the behaviour of cracked nanobeams and the factors influencing their natural frequency.

Loghmani and Yazdi [92] observed that the crack had no impact on the natural frequency of the nanobeam when it occurred at the inflexion points of the mode shapes. In contrast, Wang and Duan [141] discussed the natural frequency of nanorings/arches with a crack and discovered that the damage significantly lowers the natural frequency. Advanced manufacturing processes have played a crucial role in addressing the challenges of fabricating non-prismatic beams [44, 152, 157]. As a result, various solutions have emerged to enhance the performance of nanostructures, including stepped, tapered, sandwich, and axially graded nanostructures [20, 70, 81, 82, 89, 100, 114]. Among these solutions, stepped beams offer an economical approach by providing a larger cross-section, especially at critical segments. However, stepped beams face challenges related to complex excitation under vibration loads, potentially leading to failure. Consequently, it becomes imperative to thoroughly investigate the vibration of stepped beams using reliable and well-developed models [2, 110, 124, 131, 132]. By doing so, we can better understand their behaviour and ensure their optimal performance.

Arches' stability and structural characteristics heavily rely on the specific boundary conditions they are subjected to. These boundary conditions dictate how loads and forces are distributed throughout the arch structure, influencing its overall curved shape and support. The vibration and dynamic behaviour of arches are significantly affected by these boundary conditions, as observed by Liyvapuu and Lellep [83]. Therefore, studying the vibrations of nanoarches under different boundary conditions becomes crucial to ensure their reliable applications and avoid resonance or undesirable behaviour.

The solution of the governing equations plays a vital role in obtaining accurate results. The importance of the solution technique lies in its ability to address and solve the problem efficiently and effectively.

The method of separation of variables is applied to solve the governing differential equations in the present study. However, the current approach includes treating the nanoarch as an arch consisting of two separate contiguous segments, which are analysed independently. However, Yavari and Sarkani [153] have proposed an alternative approach by formulating the eigenvalue problem in the space of generalised functions. These generalised functions incorporate derivatives, formulating vibration and stability problems without partitioning the structural element into segments. By considering both, the influence of boundary conditions on arch behaviour and employing suitable solution techniques, a comprehensive understanding of the dynamic response and stability of nanoarches can be achieved, enhancing their practical applications.

Nanostructures, such as nanotubes, nanoplates, nanoshells, nanoarches, and nanocones etc. have exceptional mechanical and thermal properties due to their nanoscale size [34]. The discovery of CNTs led to the revelation of numerous applications of these nanotubes. CNTs serve as fundamental components in the construction of nanodevices, nanosensors and nano-oscillators [54, 66]. Consequently, researchers have extensively studied the dynamic and static behaviour of CNTs experimentally and theoretically [17, 90, 91]. Initially, vibration in CNTs was studied using classical continuum mechanics [35, 142], neglecting small scale effects such as electric forces and Van der Waals forces. However, experimental studies have shown that these small scale effects, including the lattice spacing between individual atoms, may not be neglected since the material will not be homogenized into a continuum [22]. Consequently, the nonlocal theory of elasticity is employed to study the bending, buckling and vibrations of CNTs. Here we focus on the natural frequencies of armchair, zigzag and chiral shape CNTs. The effects of cracks, nonlocal and other physical parameters on the natural frequency of CNTs are discussed.

1.2 Research scope

The main objective of this thesis is to develop a comprehensive theoretical framework that analyses the natural vibrations of curved nanobeams with defects. The ultimate goal is to enhance the safety of curved beam-type structural elements. Given the breadth of the topic, it is essential to establish the core concepts and scope of the research. In the context of structural engineering, defects refer to any deviation from the expected behaviour of a structure. Changes in material or geometric properties often lead to fluctuations in structural behaviour, affecting stiffness, mass, energy dissipation properties, and internal force distribution. A reduction in structural stiffness, for instance, alters dynamic characteristics, and if left unattended, it may eventually result in structural failure. It is crucial to clarify that this thesis focuses solely on the effects of cracks on the natural vibrations of the nanoarches in the framework of the nonlocal theory of elasticity.

Structural elements can experience various damages, such as cracks, wrinkles, foreign objects, dents, scratches, buckles, gouges, nicks, erosion, and debonding. This thesis studies the most common and potentially hazardous type: cracks. To ensure validity and comparison with alternative numerical methods, the simulation cases in this thesis adopt boundary conditions and curved nanobeam properties from existing literature. This approach helps to evaluate and validate the results effectively. The present thesis focuses on model-based methods for analysing beam deformation, displacement, and stresses. In the field of mechanics, various theories are used to study these aspects, including the Euler-Bernoulli beam theory, the Timoshenko beam theory, and the two-dimensional elastic theory. Among these theories, the Euler-Bernoulli beam theory is chosen as the foundation for this research due to its simplicity and wide applicability to long slender beams. Utilising the Euler-Bernoulli beam theory, the study investigates the natural frequencies of curved nanobeams and SWCNTs as well.

1.3 Aim of the dissertation

In this study, the natural vibrations of curved nanoarches are thoroughly investigated under different boundary conditions using semi-analytical and numerical techniques. The focus is put on finding the natural frequency of a stepped nanoarch with a stable crack. The governing equations for the investigation of the vibration of the nanoarches are derived in the framework of Eringen's nonlocal theory of elasticity. Crack-like defects introduce local compliance, which is determined by coupling the structure's local compliance with the stress intensity factor. The natural frequency of the nanoarches is then investigated under the various boundary conditions, including simply supported and clamped nanoarches, also cantilevers. The aim of the thesis is to investigate the effects of cracks, steps, and other geometrical and physical parameters on the natural frequency of nanoarches. To obtain numerical results, advanced computational tools such as MATLAB are used. Bearing in mind the challenges and expenses associated with conducting experiments at the nano level, the accuracy of the results is assessed by comparing them with existing data in the literature. Overall, the analysis of natural vibrations in curved nanoarches provides valuable insights into their behaviour and offers practical implications for engineering applications.

1.4 Contribution

The author's main contribution can be summarized as follows:

- Providing an overview of how to solve the governing differential equations with the help of the method of separation of variables.
- Providing the calculations of natural frequency parameters for various types of curved nanobeams subjected to different boundary conditions.
- Calculating the numerical results using the computer program and presenting the final results in the form of tables and figures.

- Comparing the results with those published in the literature for the validation of the method.

The solution techniques were developed in cooperation with the supervisor; the statement of the problem belongs to the supervisor.

1.5 Thesis outline

The dissertation consists of 7 chapters. Chapter 1 provides the historical background of the natural vibrations of curved nanobeams, focusing on the application of Eringen's nonlocal theory of elasticity to study the dynamic and static behaviour of the nanostructures. Chapter 2 includes the study of the physical model of the nanoarches, considering both, defects and steps, and deals with the formulation of the governing equations for analysing the natural frequency of the nanoarches. A mathematical model of the governing equations is also presented in Chapter 2. Chapter 3 discusses the natural frequency of the nanoarches of constant thickness with defect and S-S boundary conditions. In Chapter 4, the natural frequency of the S-S nanoarches of piecewise constant thickness with a defect and step is discussed. Chapter 5 focuses on the natural frequency of clamped nanoarches with both, a flaw and a step. In Chapter 6, the results of the natural frequency of cantilever nanoarches are presented. Chapter 7 includes the study of the natural frequency of the armchair, zigzag and chiral CNTs. Finally, concluding remarks are presented.

1.6 Methodology

Since conducting an extensive experimental study at the nano level is expensive, the methodology proposed in this study is based on theoretical analysis. A literature review is presented on the material properties and dimensions of nanoarches and CNTs. Governing equations based on solid mechanics principles and Eringen's non-local theory of elasticity are derived for analysing the behaviour of the natural frequency of the nanoarches. Appropriate boundary conditions were determined based on

the nature of the nanoarches under investigation. The derived equations are solved analytically. Numerical methods are employed to solve the final system of algebraic equations with the help of computer. The obtained solutions provided the natural frequencies of the nanoarches. Several physical parameters influencing the frequency are identified. The final results are compared with those existing in the literature.

Chapter 2

Physical descriptions and mathematical models

In this chapter, the governing equations of the nanoarches are derived in the framework of the nonlocal theory of elasticity and governing equations are solved analytically.

2.1 Phyical description and problem formulation

Let us consider the dynamic behaviour of a nanoarch or curved nanobeam of a piecewise constant thickness (Figure 2.1.1)

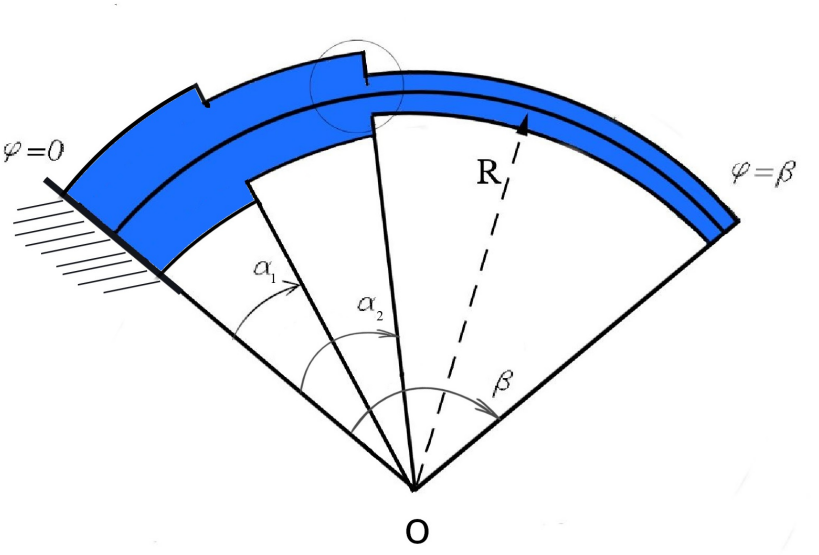

Figure 2.1.1. The geometry of the cantilever nanoarch with defects.

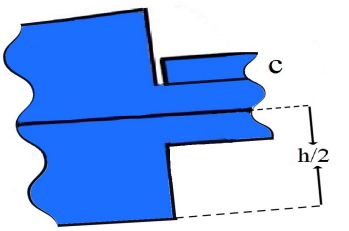

Figure 2.1.2. A flaw at the re-entrant corner of the step.

$$h = \begin{cases} h_0 \quad , \quad \varphi \in [\alpha_0, \alpha_1) \\ h_1 \quad , \quad \varphi \in (\alpha_1, \alpha_2) \\ - - - - - - - - - - - \\ h_n \quad , \quad \varphi \in (\alpha_n, \alpha_{n+1}], \end{cases}$$

where $\alpha_0 = 0$, $\alpha_{n+1} = \beta$. Let R be the radius of the nanoarch. Here h_i $(i = 0, ..., n)$ and α_j $(j = 0, ..., n+1)$ stand for given constants whereas φ is the current angle $(0 \leq \varphi \leq \beta)$. In the present thesis, the nanoarches with different end conditions are studied. However, in this section, it is assumed that the nanoarch is clamped at the left-hand end and it is absolutely free at $\varphi = \beta$. It is also assumed that at cross-sections $\varphi = \alpha_i$ stable cracks of length c_i are situated. The attention will be paid to nanoarches of rectangular cross-sections with thickness h and width $b = const$ only. The aim of the study is to elucidate the sensitivity of eigenfrequencies on the geometrical and physical parameters of the nanoarch and also on the location and length of the defects. For these purposes, the governing equations of the nonlocal theory of elasticity developed by Eringen [46] are used.

2.2 Nonlocal material behaviour

It is widely recognized that the nanomaterials subjected to the external loadings behave according to the nonlocal constitutive equations of the theory of elasticity (see Reddy [115], Eringen [46], Aydogdu [16], Ansari and Sahmani [10], Loghmani and Yazdi [92], Reddy and Pang [116], Lellep and Mubasshar [84]). In the classical theory of elasticity the stress tensor is proportional to the strain tensor at each point of the current body. However, in the nonlocal theory of elasticity the stress at the current point depends on the strain at each point of the body. Probably the simplest nonlocal constitutive equation can be presented as (see Reddy [115], Thai [134], Lellep and Lenbaum [80, 81, 82].

$$\sigma_{ij} - \eta \nabla^2 \sigma_{ij} = \sigma_{ij}^c.$$

Here σ_{ij} denotes the stress tensor for a nonlocal theory, σ_{ij}^c is the stress tensor in the classical elasticity and $\eta = (e_0 a)^2$. Here a is the dimension of the lattice of the material, e_0 stands for a material constant and ∇^2 is the nabla operator. Thus, in the nonlocal theory the stresses depend on a. If $a = 0$, the nonlocal constitutive relationship transforms into that in the classical theory of elasticity. In the present study, it is assumed that e_0

and a and, thus, also η are given constants. Evidently, the determination of η may be complicated but this is another task.

Making use of generalized stresses M (radial bending moment) and N (membrane force in the tangential direction), the nonlocal constitutive equation can be converted into

$$\begin{aligned} M - \eta\nabla^2 M &= M^c, \\ N - \eta\nabla^2 N &= N^c, \\ Q - \eta\nabla^2 Q &= Q^c, \end{aligned} \tag{2.2.1}$$

where M^c, N^c and Q^c stand for the corresponding quantities in the classical theory of elasticity (see Reddy [115], Thai [134, 135], Ansari, Rouhi and Sahmani [9], Wang et al. [144]).

It is worthwhile to mention that the total number of equations in the system (2.2.1) coincides with the number of generalized stresses necessary for the correct formulation of the current problem. In the bending problems, the dominant generalized stresses are the bending moments. In the present case according to (2.2.1) one has (s is the length of the element)

$$M - \eta\frac{\partial^2 M}{\partial s^2} = -EI_j\left(\frac{\partial^2 W}{\partial s^2} + \frac{W}{R^2}\right) \tag{2.2.2}$$

for $\varphi \in (\alpha_j, \alpha_{j+1})$; $j = 0, ..., n$. In (2.2.2) the substitution

$$M^c = -EI_j\left(\frac{\partial^2 W}{\partial s^2} + \frac{W}{R^2}\right)$$

has been introduced. Here E stands for the Young modulus and I_j is the moment of inertia of the arch in the section (α_j, α_{j+1}) and $ds = Rd\varphi$. Evidently, in the case of circular arches, the generalized stresses are the bending moment M and the membrane force N (see Soedel [129], Lellep and Lenbaum [80, 81]), also the shear force Q. Since the latter can be eliminated from the governing equations the shear force will not get any attention in the subsequent analysis. The strain components correspond-

ing N and M are (see Soedel [129]) the relative extension

$$\varepsilon = \frac{1}{R}(U^{'} + W) \tag{2.2.3}$$

and the curvature

$$\varkappa = \frac{1}{R^2}(U^{'} + W^{''}). \tag{2.2.4}$$

In (2.2.3) and (2.2.4), prims denote the differentiation with respect to the current angle, U and W denote the tangential and transverse displacements of the middle surface, respectively, and R is the radius of the arch. In the classical theory of elasticity (see Soedel [129]) it is assumed that $\varepsilon = 0$ and $U^{'} = -W$. Thus,

$$\varkappa = -\frac{1}{R}(W + W^{''}) \tag{2.2.5}$$

and

$$M^c = \frac{-Eh^3 b}{12R^2}(W + W^{''}). \tag{2.2.6}$$

The nonlocal constitutive law (2.2.2) reads as

$$M - \eta M^{''} = M^c \tag{2.2.7}$$

and

$$N - \eta N^{''} = N^c. \tag{2.2.8}$$

2.3 Equilibrium equations

The equilibrium conditions of an infinitesimal element of the arch can be presented as (see Soedel [129] and Lellep and Liyvapuu [83])

$$\begin{aligned} M^{'} - RQ &= 0, \\ N^{'} + Q + p_s R &= \rho h_j R\ddot{U}, \\ Q^{'} - N + p_n R &= \rho h_j R\ddot{W}, \end{aligned} \tag{2.3.1}$$

where $\varphi \in (\alpha_j, \alpha_{j+1})$ and $j = 0, ..., n$. Here p_s, U and p_n, W stand for

the external loads and displacements in the circumferential and normal direction, respectively. Let ρ be the density of the material and dots denote the differentiation with respect to time t and prims with respect to the length of the arch. Thus,

$$\ddot{U} = \frac{\partial^2 U}{\partial t^2}, \quad \ddot{W} = \frac{\partial^2 W}{\partial t^2}, \quad M' = \frac{\partial M}{\partial s}, \quad N' = \frac{\partial N}{\partial s}.$$

Differentiating the first equation in (2.3.1) with respect to φ and substituting it into the last one leads to the equation

$$M'' - RN + R^2(p - \rho h_j \ddot{W}) = 0, \tag{2.3.2}$$

which must be satisfied for $\varphi \in (\alpha_j, \alpha_{j+1})$.

We are considering the natural vibrations of nanoarches. Thus, it is reasonable to assume that $p_s = p_n = 0$ in (2.3.1) and $p = 0$ in (2.3.2). Making use of (2.2.3), (2.2.6), (2.2.1) and (2.3.2) one can define

$$M = \frac{-1}{R^2(1+\eta)}(EI_j(W'' + W) - h_j \eta \rho R^2 \ddot{W}) \tag{2.3.3}$$

for $\varphi \in (\alpha_j, \alpha_{j+1})$; $j = 0, ..., n$. In the following, we are looking for the solution of governing equations in the particular case when $M = -RN$. This takes place, for instance, in the case when a cantilever arch is subjected to the concentrated loading directed towards the centre of curvature of the middle line of the arch. It is assumed herein also that the membrane force vanishes. Substituting now (2.3.3) in (2.3.2) leads to the fourth-order equation

$$W^{IV} + 2W'' + W + \frac{\rho h_j R^4}{EI_j}(\eta \ddot{W}'' - \ddot{W}) = 0, \tag{2.3.4}$$

which is to be solved for $\varphi \in (\alpha_j, \alpha_{j+1})$; $j = 0, ..., n$.

2.4 Boundary conditions

Different loading and faster requirements lead to different boundary conditions to solve the governing equations of the nanoarches. These are

1. Simply supported nanoarch (S-S): In such case, the structural element is allowed for rotating but restrained translating laterally. In the case of simply supported nanoarch, the transverse displacement and bending moment must vanish at the endpoints. If β is the central angle of the nanoarch, then

$$W(0) = 0, \quad M(0) = 0, \quad W(\beta) = 0, \quad M(\beta) = 0. \tag{2.4.1}$$

2. Clamped-clamped nanoarch (C-C): In the case of clamped end conditions, the structure or system is rigidly fixed and prevents any rotation or displacement at both ends. In this case one has

$$W(0) = 0, \quad W'(0) = 0, \quad W(\beta) = 0, \quad W'(\beta) = 0. \tag{2.4.2}$$

3. Clamped-simply supported nanoarch (C-S): In the case of C-S, one end is clamped while the other end is simply supported. Thus

$$W(0) = 0, \quad W'(0) = 0, \quad W(\beta) = 0, \quad M(\beta) = 0. \tag{2.4.3}$$

4. Clamped-free (C-F) or cantilever nanoarch: In the case of cantilever nanoarch, one end is clamped, and the other is absolutely free, which means the lack of restrictions on displacement and rotation. In the case of a curved cantilever nanobeam at the free edge the bending moment and the shear force vanish. Thus,

$$M(\beta, t) = 0 \tag{2.4.4}$$

and

$$Q(\beta, t) = 0. \tag{2.4.5}$$

However, at the root section at $\varphi = 0$ one has

$$W(0,t) = 0 \tag{2.4.6}$$

and

$$W^{'}(0,t) = 0. \tag{2.4.7}$$

2.5 Cracks on the surfaces of the materials

As mentioned before in Chapter 1, cracks can appear on the surfaces of the body due to various circumstances such as environmental effects. Due to the higher surface-to-volume ratio, the nanomaterial is more susceptible to defects and cracks. In the bottom-up approach of nanomaterial formation, where materials are constructed atom by atom, atomic disorder can occur, leading to structural imperfections and surface irregularities that contribute to crack initiation. In the figure below, an electron microscope analysis of a molybdenum dioxide (MoO_2) surface reveals the presence of defects and cracks occurring at different locations on the surface.

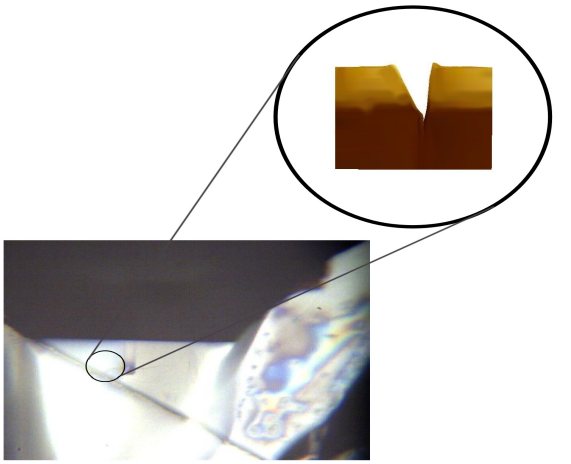

Figure 2.5.1. Crack on the surface of molybdenum dioxide.

2.6 Additional compliance due to cracks

When integrating the governing equations and also (2.3.4) one has to account for the continuity of variables $W(\varphi,t)$, $M(\varphi,t)$, $Q(\varphi,t)$ which is the consequence of physical requirements. Moreover, the slope $W^{'}(\varphi,t)$ is also continuous except at the cross-sections with defects. Let us denote

$$\theta_j = W^{'}(\alpha_j+0,t) - W^{'}(\alpha_j-0,t), \tag{2.6.1}$$

where $j = 1,...,n$. The jump of the slope of the deflection of the nanoarch is coupled with the generalized stresses at the cross-section with defects. Following Dimarogonas [37], Anifantis and Dimarogonas [8] the quantities θ_j will be treated as generalized displacements. In the linear elastic fracture mechanics, the generalized stresses P_i and generalized displacements u_i $(i = 1,...,6)$ are coupled as

$$u_i = \frac{\partial U_s}{\partial P_i}, \tag{2.6.2}$$

where U_s stands for the strain energy density. The compliance matrix with elements c_{ij} is defined as

$$c_{ij} = \frac{\partial u_i}{\partial P_j}. \tag{2.6.3}$$

Combining (2.6.2) and (2.6.3) leads to the equations

$$c_{ij} = \frac{\partial^2 U_s}{\partial P_i \partial P_j}, \tag{2.6.4}$$

where $i = 1,...,6$; $j = 1,...,n$. The total energy release rate G is defined as (see Broek [25], Anderson [7])

$$G = \frac{1-\nu^2}{E}(K_I^2 + K_{II}^2 + \frac{K_{III}^2}{1-\nu}), \tag{2.6.5}$$

whereas E is the Young modulus, ν is the Poisson ratio and

$$c_{ij} = \frac{b}{\partial P_i \partial P_j} \frac{\partial^2}{\partial P_i \partial P_j} \iint_S G\,dS. \tag{2.6.6}$$

The quantities K_I, K_{II}, K_{III} in (2.6.5) stand for the stress intensity factors corresponding to modes I, II and III, respectively (see Broek [25], Anifantis and Dimarogonas [8], Alsabbagh, Abuzeid and Dado [6]). On the other hand, the strain energy release rate can be introduced so that

$$u_i = \frac{b}{\partial P_i} \frac{\partial}{\partial P_i} \int_0^c J\,dc \tag{2.6.7}$$

and

$$c_{ij} = \frac{b}{\partial P_i \partial P_j} \frac{\partial^2}{\partial P_i \partial P_j} \int_0^c J\,dc, \tag{2.6.8}$$

where J is so-called $J-integral$ of Rice (see Rice [118]). It is worth to emphasize that dc stands in (2.6.7)-(2.6.8) for the extension of the crack and c_{ij} are corresponding compliances due to the crack. Note that the energy release rate G was originally introduced for the characterization of the energy behaviour in the neighbourhood of the crack tip in linear

elastic materials. However, Rice [118] was able to extend the energy release rate to non-linear materials. He showed that the non-linear energy release rate can be expressed as a line integral called $J-integral$. The $J-integral$ is evaluated along an arbitrary closed contour Γ around the crack tip. It is defined as (see Broek [25], Anderson [7])

$$J=\int_{\Gamma}(U_s\,dy-T_i\frac{\partial u_i}{\partial x}\,ds). \tag{2.6.9}$$

In (2.6.9), T_i stand for external forces (tractions) and Γ is a closed contour followed counterclockwise. Consider now a particular case when at $\varphi=\alpha_j$ a mode I crack is located. If θ_j is treated as a generalized coordinate then the generalized forces associated with θ_j are $M_j=M(\alpha_j,t)$ and $N_j=N(\alpha_j,t)$. Thus

$$\theta_j=C_{0j}\overrightarrow{Q}(\alpha_j,t), \tag{2.6.10}$$

where $\overrightarrow{Q}$ is the vector with coordinates $M(\alpha_j,t),N(\alpha_{j,t})$ and C_{0j} stands for the corresponding line of the compliance matrix. It is reasonable to introduce the notation

$$C_{ij}=\begin{bmatrix}c_{11}(\alpha_{j,t}) & c_{12}(\alpha_{j,t})\\ c_{21}(\alpha_{j,t}) & c_{22}(\alpha_{j,t})\end{bmatrix}. \tag{2.6.11}$$

Due to symmetry $c_{12}=c_{21}$ at each α_j. It is worthwhile to mention that the local stiffness K_j is reciprocal to the local compliance c_j in the one-dimensional case (see Lellep and Sakkov [85]). An alternative case is studied by Anifantis and Dimarogonas [8]. It is known from the linear elastic fracture mechanics that (see Broek [25] Anderson [7], Broberg [24])

$$G=\frac{M^2}{2b}\frac{dC}{dc} \tag{2.6.12}$$

if a beam element is subjected to the bending moment M. Here C is the compliance and c stands for the crack length. In this case the stress intensity factor is

$$K=\frac{\sigma M}{bh^2}\sqrt{\pi c}F_1(\frac{c}{h}). \tag{2.6.13}$$

In (2.6.13), F_1 stands for so-called shape function which must be determined experimentally, h being the thickness. However, there exist rich databases (see Tada et al. [133]) which can be used for the interpolation of shape functions $F_1(s)$ and $F_2(s)$ (here $s = c/h$). If the beam element is loaded with the moment M_j and the tensile force N_j then the stress intensity coefficient is calculated as (see Tada et al. [133], Zhou and Huang [158])

$$K_j = \frac{\sqrt{\pi s_j}}{b\sqrt{h}}(N_j F_1(s_j) + \frac{6M_j}{h} F_2(s_j)), \tag{2.6.14}$$

where

$$F_1 = 1.12 - 0.23s + 10.55s^2 - 21.72s^3 + 30.39s^4 \tag{2.6.15}$$

and

$$F_2 = 1.12 - 1.4s + 7.33s^2 - 13.08s^3 + 14.08s^4. \tag{2.6.16}$$

In (2.6.14), the quantity h can be interpreted as $h = min(h_j, h_{j+1})$. Another type of the shape function can be presented as (see Tada et al. [133])

$$F(s) = \sqrt{\frac{2}{\pi s}\tan\frac{\pi s}{2}} \cdot \frac{0.923 + 0.199(1 - \sin\frac{\pi s}{2})^4}{\cos\frac{\pi s}{2}}. \tag{2.6.17}$$

Making use of the shape functions (2.6.15)-(2.6.17) one can calculate the elements of the compliance matrix (2.6.11)

$$\begin{aligned} c_{11}(\alpha_j) &= \frac{2}{Eb}\int_0^c sF_1^2\,ds, \\ c_{12}(\alpha_j) &= \frac{2}{Ebh}\int_0^c sF_1F_2\,ds, \\ c_{22}(\alpha_j) &= \frac{2}{Eb}\int_0^c sF_2^2\,ds. \end{aligned} \tag{2.6.18}$$

Finally, making use of (2.6.18) one can calculate

$$\theta_j = c_{11}(\alpha_j)M(\alpha_j,t) + c_{12}(\alpha_j)N(\alpha_j,t) \tag{2.6.19}$$

and the corresponding displacement

$$\delta_j = c_{21}(\alpha_j)M(\alpha_j,t) + c_{22}(\alpha_j)N(\alpha_j,t). \tag{2.6.20}$$

2.7 Solution of the governing equations

In order to solve the equation (2.3.4) in regions $(\alpha_j, \alpha_{j+1});\ j = 0,...,n$ the method of separation of variables is applicable. Assume, thus, that

$$W(\varphi,t) = X_j(\varphi)T(t) \tag{2.7.1}$$

for $\varphi \in (\alpha_j, \alpha_{j+1});\ j = 0,...,n$. The transformation (2.7.1) admits to present (2.3.4) as the system of equations consisting of

$$\ddot{T} + \omega^2 T = 0 \tag{2.7.2}$$

and

$$X_j^{IV} + X_j^{''}(2 + A_j\eta) + X_j(1 - A_j) = 0, \tag{2.7.3}$$

where

$$A_j = \frac{\omega^2 \rho h_j R^4}{EI_j}; j = 0,...,n. \tag{2.7.4}$$

The characteristic equation for the linear fourth-order equation (2.7.3) is

$$\lambda_j^4 + (2 + A_j\eta)\lambda_j^2 + 1 - A_j = 0; j = 0,...,n. \tag{2.7.5}$$

It immediately follows from (2.7.5) that

$$\lambda_j^2 = \frac{1}{2}(-2 - A_j\eta) \pm \frac{1}{2}\sqrt{(2 + A_j\eta)^2 - 4(1 - A_j)} \tag{2.7.6}$$

and the general solution of (2.3.4) has the form

$$X_j = C_{1j}\cosh\mu_j\varphi + C_{2j}\sinh\mu_j\varphi + C_{3j}\cos\nu_j\varphi + C_{4j}\sin\nu_j\varphi, \quad (2.7.7)$$

where $j = 0,\ldots,n$ and

$$\mu_j = \sqrt{-1 - \frac{\eta}{2}A_j + B_j} \quad (2.7.8)$$

and

$$\nu_j = \sqrt{1 + \frac{\eta}{2}A_j + B_j}, \quad (2.7.9)$$

where the notation

$$B_j = \frac{1}{2}\sqrt{A_j^2\eta^2 + 4A_j(1+\eta)} \quad (2.7.10)$$

is introduced. Note that the solution of the equation (2.7.2) depending on time can be presented as

$$T = \sin(\omega t), \quad (2.7.11)$$

ω being the natural frequency of the nanoarch. Evidently, now

$$W(\varphi,0) = 0, \quad \dot{W}(\varphi,0) = \omega X_j(\varphi) \quad (2.7.12)$$

for $\varphi \in (\alpha_j, \alpha_{j+1})$; $j = 0,\ldots,n$. It is presumed herewith that the initial conditions are given in the form (2.7.12). Consider now the boundary conditions. At the root section $\varphi = 0$ according to (2.4.6), (2.4.7) and (2.7.1), one has

$$X_0(0) = 0, \quad X_0^{'}(0) = 0. \quad (2.7.13)$$

The boundary conditions corresponding to the free edge are presented by (2.4.4) and (2.4.5). Making use of (2.3.3) and (2.7.1) one can check that the requirements at the free edge are satisfied if

$$X_n^{''}(\beta) + X_n(\beta)(1+A_n) = 0 \quad (2.7.14)$$

and

$$X_n^{'''}(\beta)+X_n^{'}(\beta)(1+A_n)=0. \tag{2.7.15}$$

2.8 Intermediate jump conditions

It was stated above that due to cracks the nanoarch has additional flexibility. The additional compliance can be calculated by making use of the relations (2.6.10)-(2.6.20). According to this concept, the slope $W^{'}$ has finite jumps $[W^{'}(\alpha_j)]$ at $\varphi=\alpha_j$ $(j=1,...,n)$. Thus

$$W^{'}(\alpha_j+0,t)=W^{'}(\alpha_j-0,t)+\theta_j, \tag{2.8.1}$$

where θ_j is evaluated by (2.6.10), (2.6.11). Making use of (2.3.3), (2.7.1), one can present

$$M(\alpha_j+0,t)=\frac{-EI_j}{(1+\eta)R^2}(X_j^{''}(\alpha_j)+(1+A_j\eta)X_j(\alpha_j)T(t). \tag{2.8.2}$$

In (2.8.1), (2.8.2) one has to distinguish the left-hand and right-hand limits, respectively. Here the notation

$$g(\alpha\pm 0)=\lim_{x\to\alpha\pm 0} g(x) \tag{2.8.3}$$

is used. It follows from (2.6.1), (2.6.10)-(2.6.19) that

$$\theta_j=(c_{11}(\alpha_j)-\frac{c_{12}(\alpha_j)}{R})M(\alpha_j,t), \tag{2.8.4}$$

where the compliances $c_{11}(\alpha_j)$ and $c_{12}(\alpha_j)$ are evaluated by (2.6.18). It is evident from the physical considerations that the stress components $M(\varphi,t)$ and $Q(\varphi,t)$ together with the displacement $W(\varphi,t)$ must be continuous at each time instant at each $\varphi\in(0,\beta)$. Thus, the set of continuity and jump conditions is

$$[W(\alpha_j,t)]=0,\quad [W^{'}(\alpha_j,t)]=\theta_j,\quad [M(\alpha_j,t)]=0,\quad [Q(\alpha_j,t)]=0, \tag{2.8.5}$$

$j = 1, ..., n$. Here the notaion

$$[X(\alpha)] = X(\alpha + 0) - X(\alpha - 0)$$

is used.

Chapter 3

Natural frequency of the simply supported nanoarches of constant thickness

In this chapter, the natural frequency for the first mode of the nanoarches of constant thickness is discussed. The nanoarches considered in this section are simply supported and also have a crack-like defect.

3.1 Physical description

The geometry of a S-S nanoarch with a defect is shown in Figures 3.1.1 and 3.1.2. Here h is the thickness and R is the radius of the arch. If we use polar coordinates, the current cross-section is defined by φ, and the edges of the arch correspond to $\varphi = 0$ and $\varphi = \beta$. It is assumed that a stable crack whose length is $c < h$ is located at $\varphi = \alpha$. It is also assumed that the cross-section of the nanoarch is rectangular.

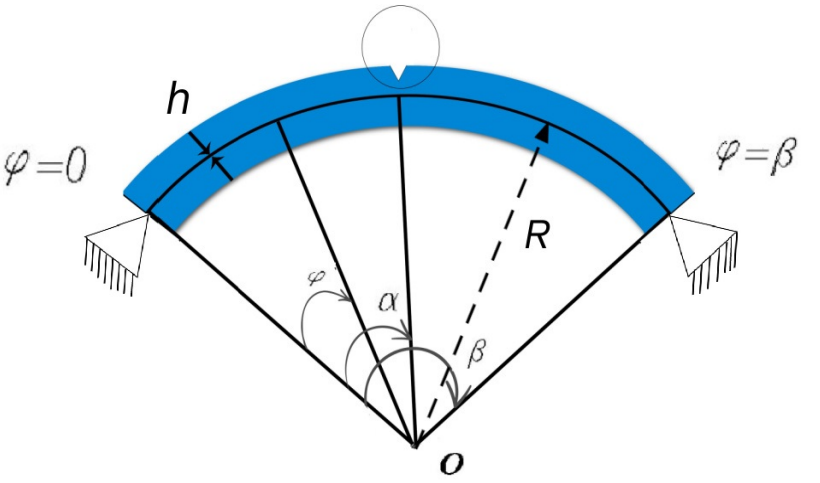

Figure 3.1.1. Geometry of the nanoarch of a constant thickness with a crack.

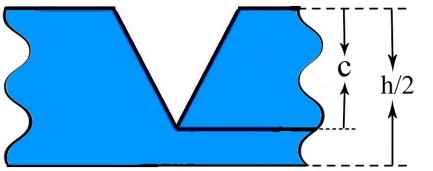

Figure 3.1.2. Crack in the nanoarch at $\varphi = \alpha$.

By using (2.4.1) in the general solution (2.7.7) we immediately get $C_{10} = C_{30} = 0$ and (2.7.7) takes the shape

$$w = \begin{cases} C_{20}\sinh\mu_0\varphi + C_{40}\sin\nu_0\varphi & ; \quad \varphi \in (0,\alpha) \\ A\sinh\mu_1(\varphi-\beta) + C\sin\nu_1(\varphi-\beta); & \varphi \in (\alpha,\beta) \end{cases} \tag{3.1.1}$$

where

$$A = \frac{-C_{11}}{\sin \mu_1 \beta}, \quad C = \frac{-C_{13}}{\sin \nu_1 \beta}.$$

We get a system of four linear homogeneous equations by satisfying the boundary and the intermediate conditions in (3.1.1). The result can be written as

$$\begin{aligned}
&(\sinh(\mu_0\alpha)C_{20} + \sin \nu_0\alpha C_{40} - A\sinh(\mu_1(\alpha-\beta)) + \\
&C\sin(\nu_1(\alpha-\beta)) = 0, \\
&(\mu_0 \cosh(\mu_0\alpha) + p(1+\mu_0^2)\sinh(\mu_0\alpha))C_{20} - \\
&\left(\nu_0\cos(\nu_0\alpha) + p(1-\nu_0^2)\sin(\nu_0\alpha)\right)C_{40} + \\
&C\sin(\nu(\alpha-\beta)) + A\mu_1\cosh(\mu_1(\alpha-\beta)) + C\nu_1(\alpha-\beta) = 0, \\
&C_{20}\mu_0^2\sinh(\mu_0\alpha) - C_{40}\nu_0^2\sin(\nu_0\alpha) - \\
&A\mu_1^2\sinh(\mu_1(\alpha-\beta)) + C\nu_1^2\sin(\nu_1(\alpha-\beta)) = 0, \\
&C_{20}\mu_0^3\cosh(\mu_0\alpha) - C_{40}\nu_0^3\cos(\nu_0\alpha) - \\
&A\mu_1^3\cosh(\mu_1(\alpha-\beta)) + C\nu_1^3\cos(\nu_1(\alpha-\beta)) = 0.
\end{aligned}$$

Based on the linear homogeneous system of the above four algebraic equations with the unknowns $C_{20}, C_{40}, C_{11}, C_{13}$, we can determine its non-trivial solution by examining the determinant $\triangle$. This system has a non-trivial solution if and only if its determinant $\triangle$ equals to zero.

3.2 Numerical results and discussion

Numerical results are presented for nanoarches of constant thickness and simply supported at both ends. The nanoarches have no step and the material constants are $E = 7 \times 10^{11}\ Pa$, $\nu = 0.3$, $\eta = 1\ nm$ and $R = 80\ nm$. It is assumed that $\beta = 1\ rad$. The wall thickness is $h_0 = h_1 = 10\ nm$. In Figure 3.2.1, the natural frequency is plotted against the radius of the nanoarches. It is evident from the figure that the frequency decreases as the radius increases. The different curves in Figure 3.2.1 correspond to various defect locations. Furthermore, the figure illustrates that the location of the defects also influences the natural frequency. Figure 3.2.2

displays the natural frequency plotted against the nonlocal parameter. The behaviour of the frequency indicates that a lower value of the nonlocal parameter results in a higher frequency. The curves in the figure correspond to different values of the central angle of the nanoarch. It can be seen from the figure that as the central angle increases, the natural frequency also increases. The results obtained for the constant thickness of the nanoarch are compared with those obtained by Hosseini and Rahmani [63] in Table 3.2.1. Table 3.2.1 shows that the results are in reasonable correspondence.

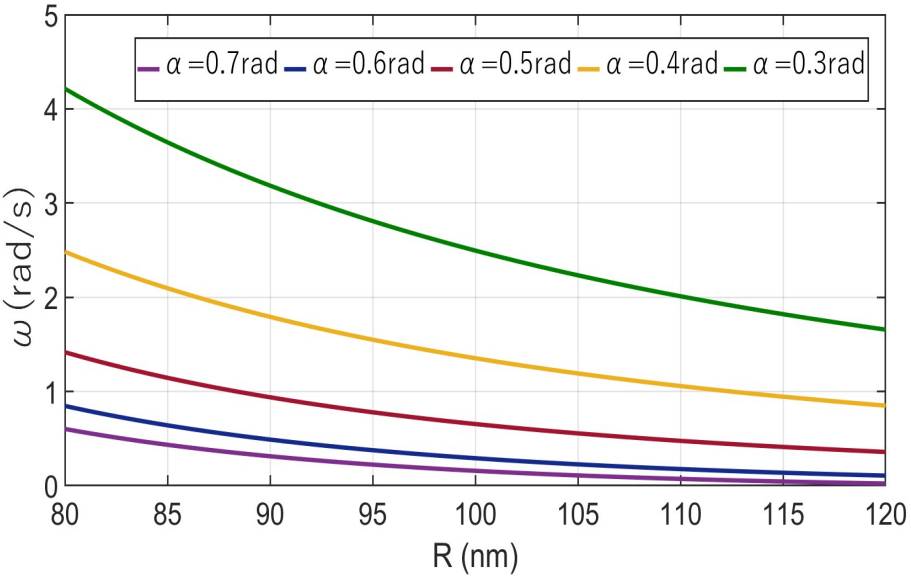

Figure 3.2.1. Natural frequency versus radius of the nanoarch.

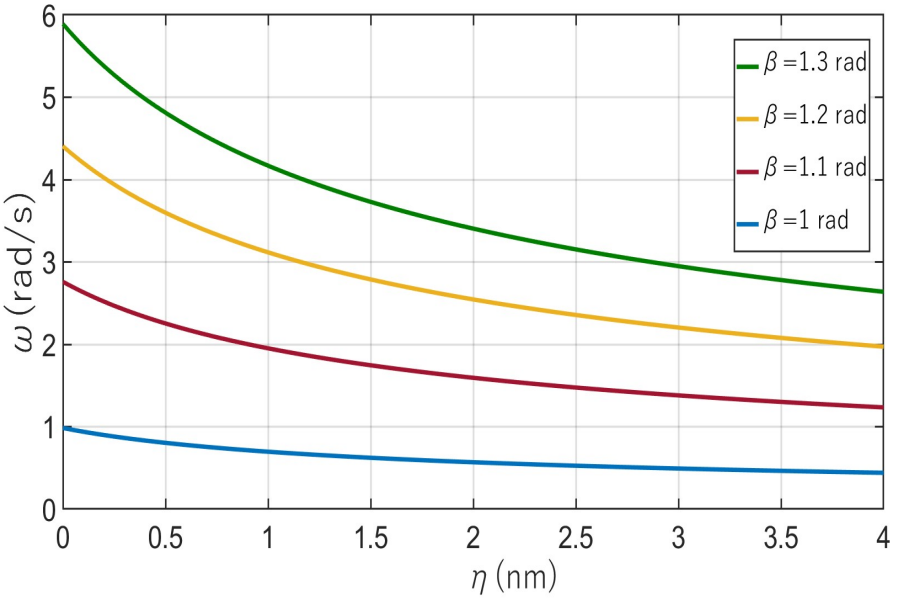

Figure 3.2.2. Natural frequency versus nonlocal parameter.

Table 3.2.1. Natural vibration of the nanoarches of constant thickness .

Mode	η (nm)	Present	Hosseini and Rahmani [63]
1	0	8.10582	8.1991
	1	7.50558	7.8222
	2	7.00188	7.4929
	3	6.74192	7.2020
	4	6.31883	6.9425

Chapter 4

Natural frequency of the simply supported nanoarches of piecewise constant thickness

This chapter analyses the natural frequency of the nanoarches of piecewise constant thickness. The effects of cracks and steps are also recorded and drawn in the different figures. The frequencies of the nanoarches with a step are compared with those corresponding to nanoarches of constant thickness.

4.1 Description of the problem

Let us consider the dynamic behaviour of a nanoarch shown in Figure 4.1.1. It is assumed that the thickness of the nanoarch is defined as

$$h = \begin{cases} h_0 & , \quad \varphi \in [0, \alpha) \\ h_1 & , \quad \varphi \in (\alpha, \beta]. \end{cases} \tag{4.1.1}$$

In (4.1.1), h_0, h_1 are given numbers and $\alpha \in (0, \beta)$. The width b of the nanoarch is assumed to be a constant. The study aims to determine the

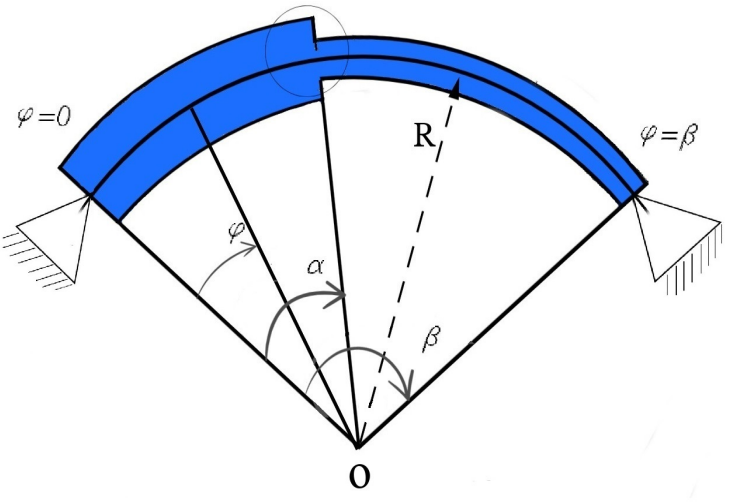

Figure 4.1.1. Simply supported stepped nanoarch with a defect.

eigenfrequencies of stepped nanobeams weakened with defects at the re-entrant corners of steps. It is assumed that at the cross-section $\varphi = \alpha$, a crack with length c is located. The defect is treated as a stable crack; no attention will be paid to the extension of the crack during vibrations. However, the sensitivity of the eigenfrequency with respect to the position of the crack and other parameters will be clarified. The boundary conditions (2.4.1) and the general solution (2.7.7) are used in order to get numerical results. We get a system of four linear algebraic equations with four unknowns whose coefficients can be written in the form of a matrix. The system of equations has a non-trivial solution if and only if its determinant $\triangle$ equals zero. The determinant

$$\triangle = \begin{vmatrix} K_{11} & K_{12} & K_{13} & K_{14} \\ K_{21} & K_{22} & K_{23} & K_{24} \\ K_{31} & K_{32} & K_{33} & K_{34} \\ K_{41} & K_{42} & K_{43} & K_{44} \end{vmatrix},$$

here the elements of the determinant $\triangle$ are following:

$$
\begin{aligned}
K_{11} &= \sinh(\mu_0\alpha);\\
K_{12} &= \sin(\nu_0\alpha);\\
K_{13} &= -(\sinh(\mu_1\alpha) - \tanh(\mu_1\beta)\cosh(\mu_1\alpha));\\
K_{14} &= -(\sin(\nu_1\alpha) - \tan(\nu_1\beta)\cos(\nu_1\alpha));\\
K_{21} &= -\mu_0\cosh(\mu_0\alpha);\\
K_{22} &= -\nu_0\cos(\nu_0\alpha);\\
K_{23} &= \mu_1(\cosh(\mu_1\alpha) - \tanh(\mu_1\beta)\sinh(\mu_1\alpha))\\
&\quad -p(\mu_1^2+1)(\sinh(\mu_1\alpha) - \tanh(\mu_1\beta)\cosh(\mu_1\alpha));\\
K_{24} &= \nu_1(\cos(\nu_1\alpha) + \tan(\nu_1\beta)\sin(\nu_1\alpha))\\
&\quad -p(1-\nu_1^2)(\sin(\nu_1\alpha) - \tan(\nu_1\beta)\cos(\nu_1\alpha));\\
K_{31} &= \mu_0^2\sinh(\mu_0\alpha);\\
K_{32} &= -\nu_0^2\sin(\nu_0\alpha);\\
K_{33} &= -\mu_1^2(\sinh(\mu_1\alpha) - \tanh(\mu_1\beta)\cosh(\mu_1\alpha));\\
K_{34} &= -\nu_1^2(\tan(\nu_1\beta)\cos(\nu_1\alpha) - \sin(\nu_1\alpha));\\
K_{41} &= \mu_0^3\cosh(\mu_0\alpha);\\
K_{42} &= -\nu_0^3\cos(\nu_0\alpha);\\
K_{43} &= -\mu_1^3(\cosh(\mu_1\alpha) - \tanh(\mu_1\beta)\sinh(\mu_1\alpha));\\
K_{44} &= \nu_1^3(\cos(\nu_1\alpha) + \tan(\nu_1\beta)\sin(\nu_1\alpha)).
\end{aligned}
$$

4.2 Numerical results and discussion

Natural frequencies for the first mode are presented for nanoarches simply supported at both ends in Figures 4.2.1-4.2.6. Here the nanoarches have a single step and the material constants are $E = 7 \times 10^{11}\ Pa$, $\nu = 0.3$, $\eta = 1\ nm$ and $R = 30\ nm$. It is assumed that $\beta = 1\ rad$ if β is not specified in the legend. The wall thickness is $h_0 = 10\ nm$. However, $h_1 = 20\ nm$ except in Figure 4.2.1.

In Figure 4.2.1, the natural frequency of the nanoarch versus the thickness h_1 is depicted for different values of the radius R. It can be seen from Figure 4.2.1 that the natural frequency increases if the thickness of the arch increases. However, if the radius of the arch increases, then the natural frequency decreases.

In Figures 4.2.2 and 4.2.3, the natural frequency as a function of the step location α is presented. In Figure 4.2.2, the nanoarch with the central angle $\beta = 1\ rad$ is treated. Different curves in Figure 4.2.2 correspond to the crack extensions $s = 0$, $s = 0.1$, $s = 0.2$, $s = 0.3$, $s = 0.4$ respectively. It can be seen from Figure 4.2.2 that the lowest natural frequency values correspond to the arch without any cracks. In Figure 4.2.3, similar results are presented for different values of the central angle β (here $s = 0.7$). It reveals from Figure 4.2.3 that in the case of smaller values of the angle α, the lowest eigenfrequency is achieved in the case of the largest value of the central angle β. However, in the case when $\beta > 2\alpha$, this relationship is more complicated. The relationship between the natural frequency and the radius R of the nanoarch is shown in Figure 4.2.4 in the case $\beta = 1\ rad$ and $s = 0.7$ (here $\eta = 1\ nm$).
It reveals from Figure 4.2.4 that the smaller is α, the larger is the natural frequency of the nanoarch. On the other hand, the larger α, the lower is the eigenfrequency. The dependence of the eigenfrequency on the material parameter $\eta = (e_0 a)^2$ is demonstrated in Figure 4.2.5 for different values of the radius R. Generally speaking, the eigenfrequency decreases if the material parameter increases. Thus, in the case $\eta = 0$, the natural frequency has its maximal value.
The sensitivity of the eigenfrequency on the central angle β of the nanoarch is shown in Figure 4.2.6 for the radius $R = 30\ nm$. Different curves in

Figure 4.2.6 correspond to nanoarches having the step in different cross sections (here $\eta = 1\ nm$). One can see from Figure 4.2.6 that in the case of larger values of the angle β, curves corresponding to different values of the step angle are quite close to each other. However, if $\beta < 0.6\ rad$, the discrepancies between these curves are large.

The results obtained in the current study are compared with those obtained by Thai [134] when $\alpha = 0\ rad$, $\beta = 0.008\ rad$. Table 4.2.1 shows that the results are in reasonable correspondence. One can see from Table 4.2.1 that the results are close to each other for small values of η but for larger values of η the discrepancy between corresponding results is larger. Table 4.2.2 compares the frequencies of nanoarches with step and without step. It can be seen from Table 4.2.2 that the frequencies of nanoarches with step are higher than those without step for the first and second modes.

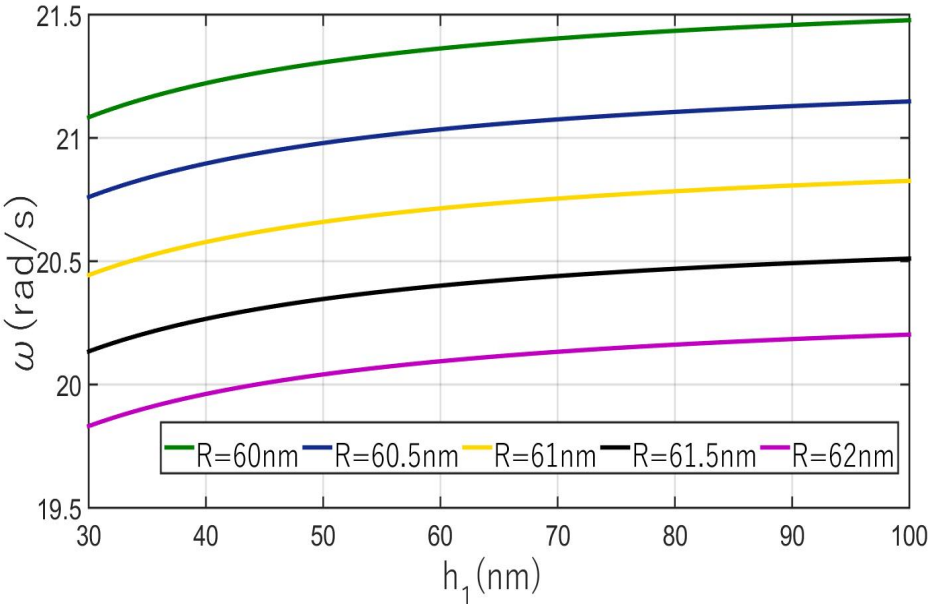

Figure 4.2.1. Natural frequency versus the thickness of the nanoarch.

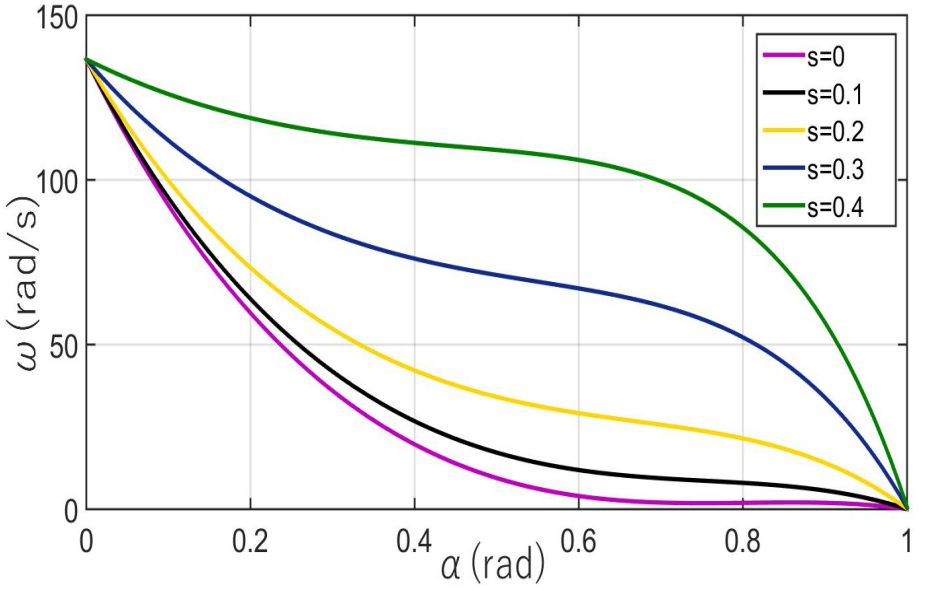

Figure 4.2.2. Natural frequency versus defect location.

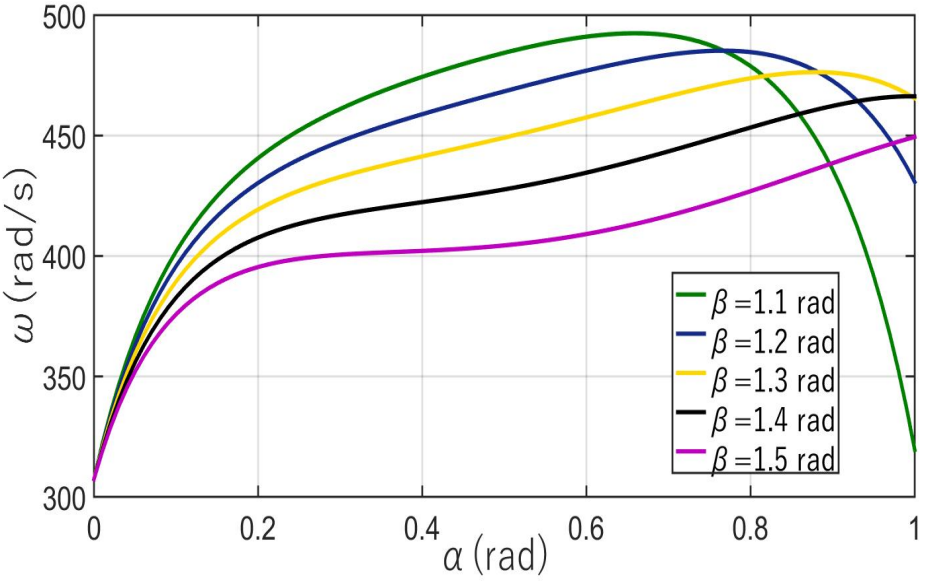

Figure 4.2.3. Natural frequency versus defect location for different angles β.

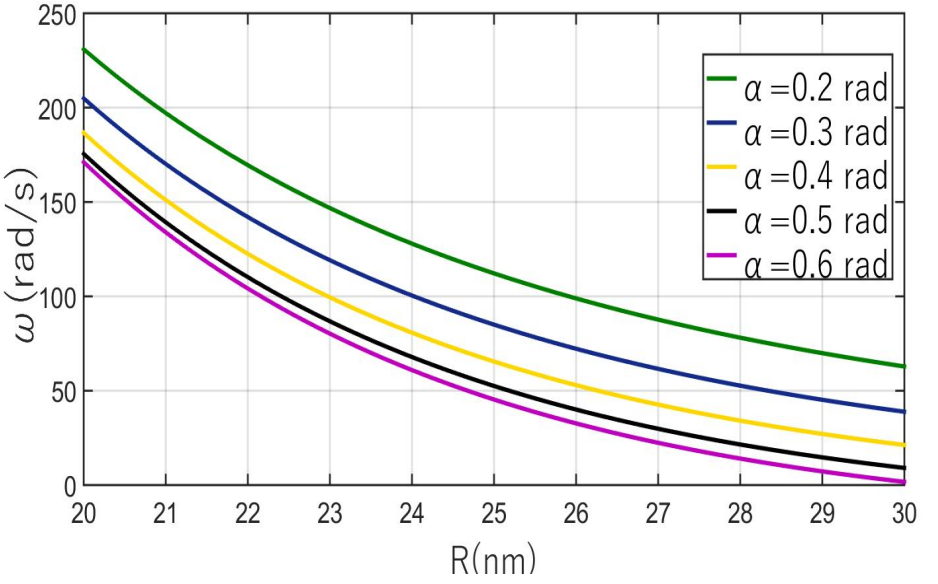

Figure 4.2.4. Natural frequency versus radius of the nanoarch.

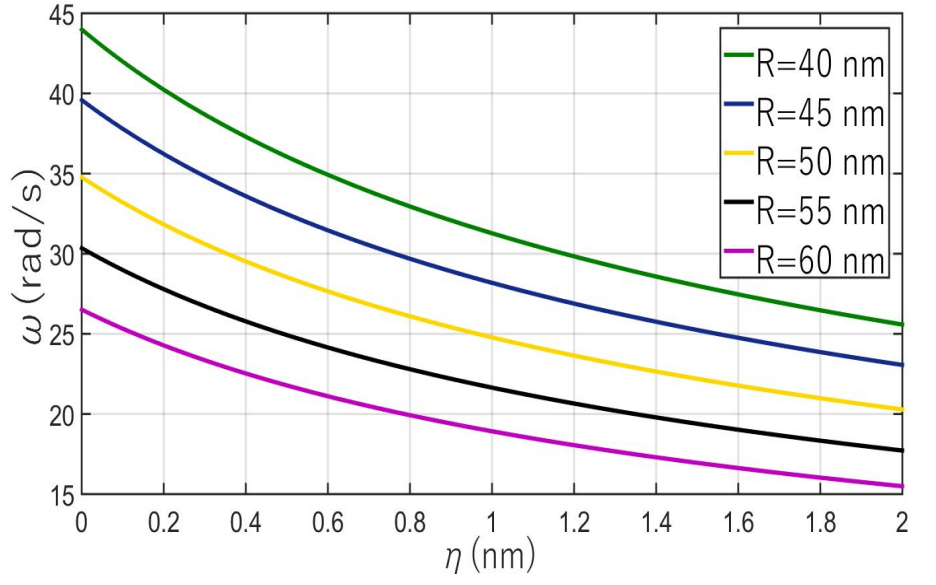

Figure 4.2.5. Natural frequency versus nonlocal parameter.

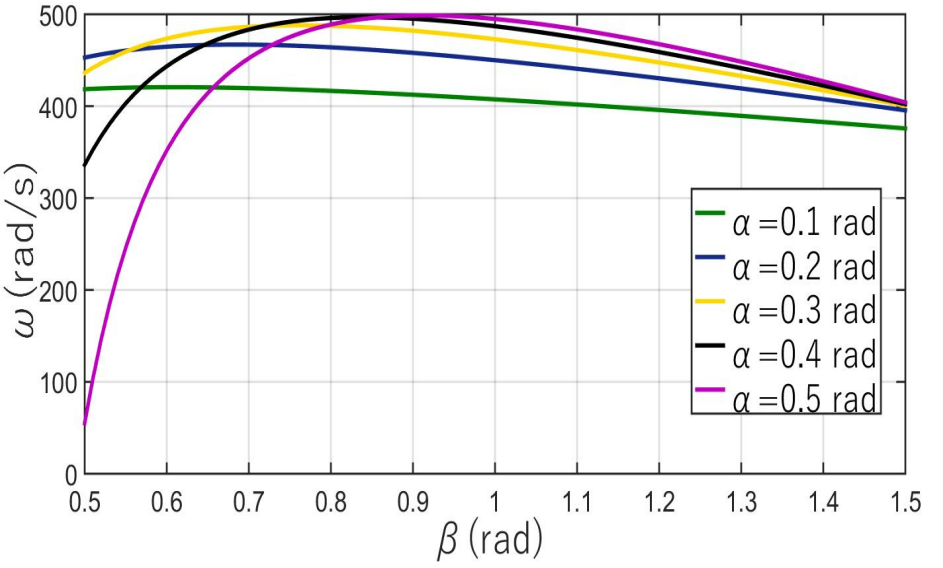

Figure 4.2.6. Natural frequency versus central angle.

Table 4.2.1. Natural vibration of the nanoarches of the constant thickness.

Mode	η (nm)	Present	Thai [134]
1	0	9.75821	9.2745
	1	7.05584	8.8482
	2	5.80188	8.4757
	3	5.04192	8.1466
	4	4.51883	7.8530

Table 4.2.2. Simply supported nanoarches .

Mode	η (nm)	With step	Without step
1	0	6.29953	5.76223
	1	4.47050	4.07838
	2	3.65442	3.33093
	3	3.16666	2.88507
	4	2.83332	2.58069
2	0	17.56912	15.45628
	1	15.45783	13.54736
	2	14.13590	12.40031
	3	13.99210	11.44508
	4	12.73064	10.46135

Chapter 5

Natural frequency of clamped nanoarches

In this chapter, the natural frequency of clamped nanoarches is discussed. The arch has a step and a crack at the re-entrant corner of the step. The natural frequencies of S-S and C-C nanoarches are calculated.

5.1 Problem description

The problem is formulated as we did in the case of simply supported nanoarches. In this section, the nanoarch is clamped at both ends, as shown in Figure 5.1.1. In order to find the natural frequency of the nanoarches clamped at both ends, the general solution (2.7.7) is used for the boundary conditions (2.4.2).

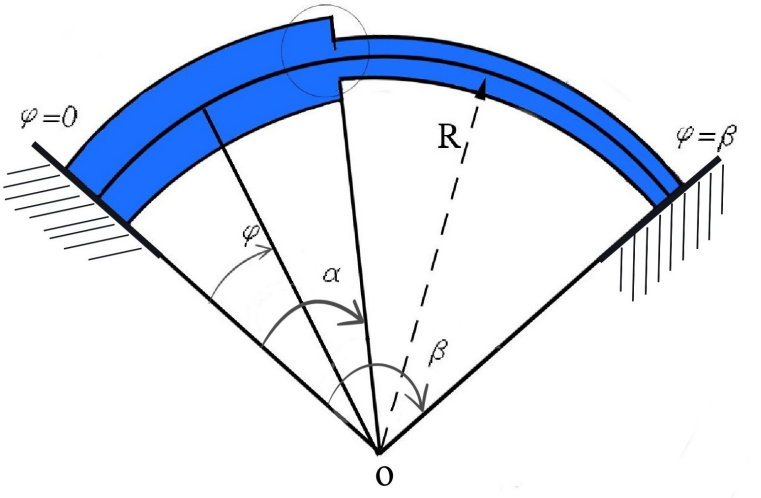

Figure 5.1.1. Clamped nanoarch with a step.

5.2 Results and discussion

The main objective of the analysis is to define the natural frequency of the clamped nanoarch with defects and to study how the different parameters affect the natural frequency. Here the nanoarch with a single step is considered. Natural frequencies for the first mode are presented for nanoarches clamped at both ends in Figures 5.2.1-5.2.5. Material properties used to draw the figures are; $E = 7 \times 10^{11}\ Pa$, $h_0 = 10\ nm$, $h_1 = 20\ nm$, $\rho = 10\ kg/m^3$, $b = 1\ nm$. The radius of the arch $R = 110\ nm$ except in Figures 5.2.4 and 5.2.5. Material constant $\eta = 3\ nm$ in Figures 5.2.2 and 5.2.4. The shape function given in the equation (2.6.15) is used to draw the Figures 5.2.1-5.2.5. In Figure 5.2.1, the natural frequency of the nanoarch versus central angle is drawn by considering different values of the material constant. It is clear from Figure 5.2.1 that natural frequency increases as the central angle β increases. However, the natu-

ral frequency decreases if the material constant η increases.

In Figure 5.2.2, the natural frequency versus the central angle β is depicted for different values of the depth of the crack in the nanoarch. It can be seen from Figure 5.2.2 that the crack's depth significantly affects the natural frequency. The natural frequency keeps decreasing as the depth of the crack is increasing. Nonetheless, the effect of β on natural frequency is similar to that shown in Figure 5.2.1. Different curves in Figure 5.2.2 correspond to the crack extensions $s = 0$, $s = 0.2$, $s = 0.4$, $s = 0.6$ and $s = 0.8$, respectively. It can be seen from Figure 5.2.2 that the highest value of the natural frequency corresponds to the arch without any cracks, that is, $s = 0$. In Figure 5.2.3, the natural frequency is depicted versus the material constant η. It is revealed from the figure that natural frequency decreases as we increase the material constant η. However, the natural frequency decreases as the radius R increases.

The relationship between the natural frequency and the radius R of the nanoarch is shown in Figure 5.2.4 by taking into account the crack location α. The considerable changes in the natural frequency are noted for different locations of the crack of the nanoarch. It is also clear from Figure 5.2.4 that the natural frequency decreases if the radius of the nanoarch increases.

The natural frequencies for two different shape functions are compared in Figure 5.2.5. In Figure 5.2.5, f and f* denote the frequencies calculated by using shape functions given by (2.6.15) and (2.6.17), respectively.

The present study's results are compared with those of other authors. In Table 5.2.1, the natural frequencies of the nanoarches for the first and second modes are compared with the results by Ganapathi et al. [50]. It can be seen from Table 5.2.1 that the results obtained above are in good correlation with the results of Ganapathi et al. [50]. In Table 5.2.2, the natural frequencies of simply supported and clamped nanoarches are compared. The table shows that the natural frequency of clamped nanoarches is higher than that of the simply supported nanoarches.

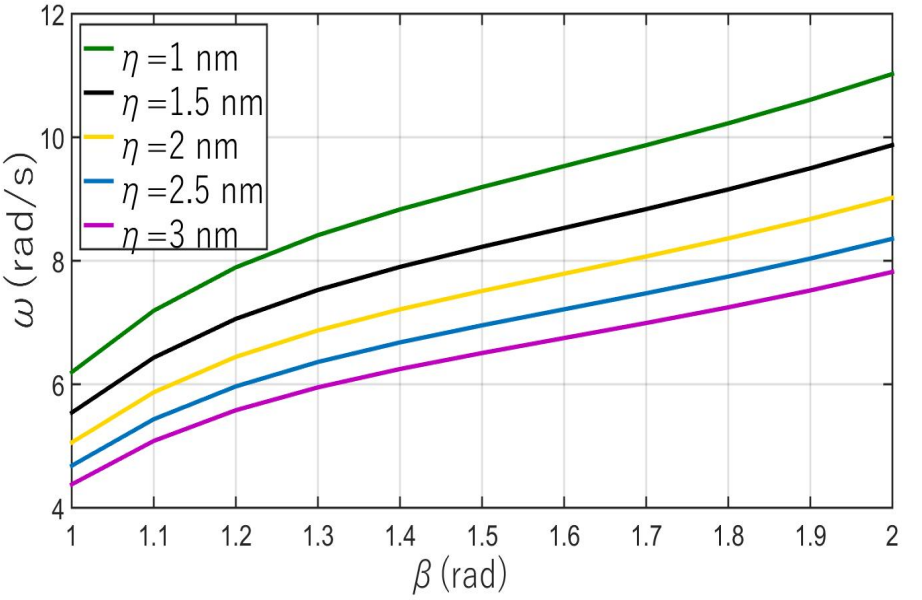

Figure 5.2.1. Natural frequency versus central angle of the nanoarch.

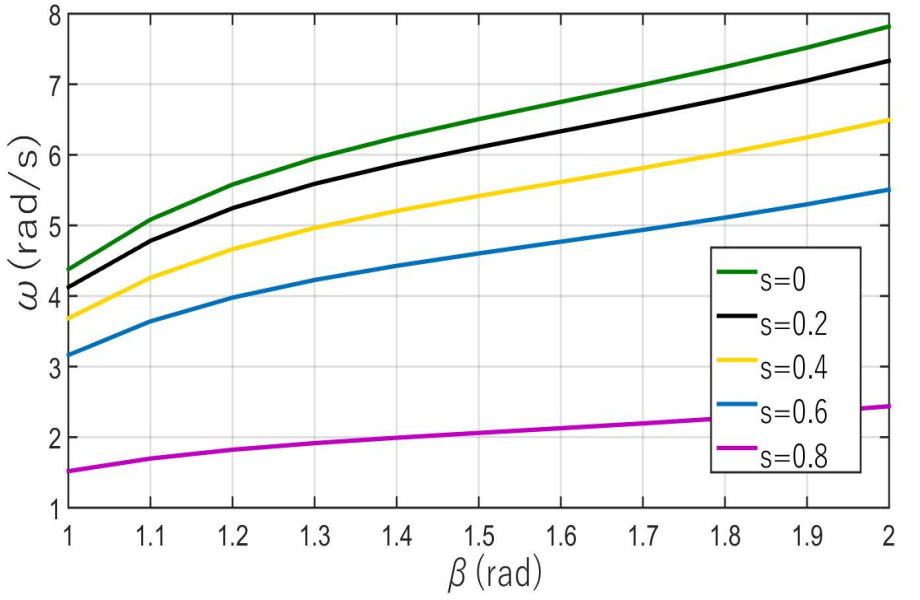

Figure 5.2.2. Natural frequency versus central angle of the nanoarch.

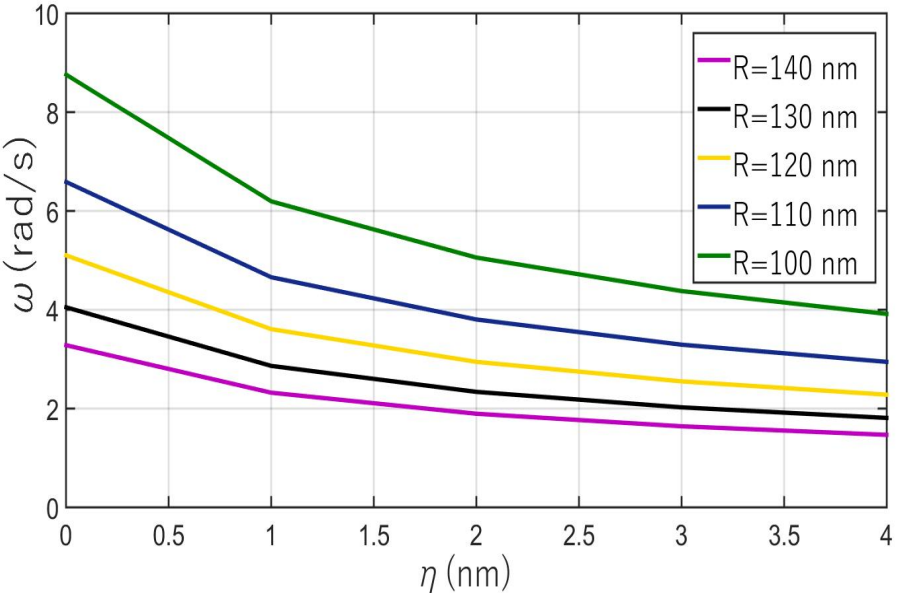

Figure 5.2.3. Natural frequency of stepped nanoarches.

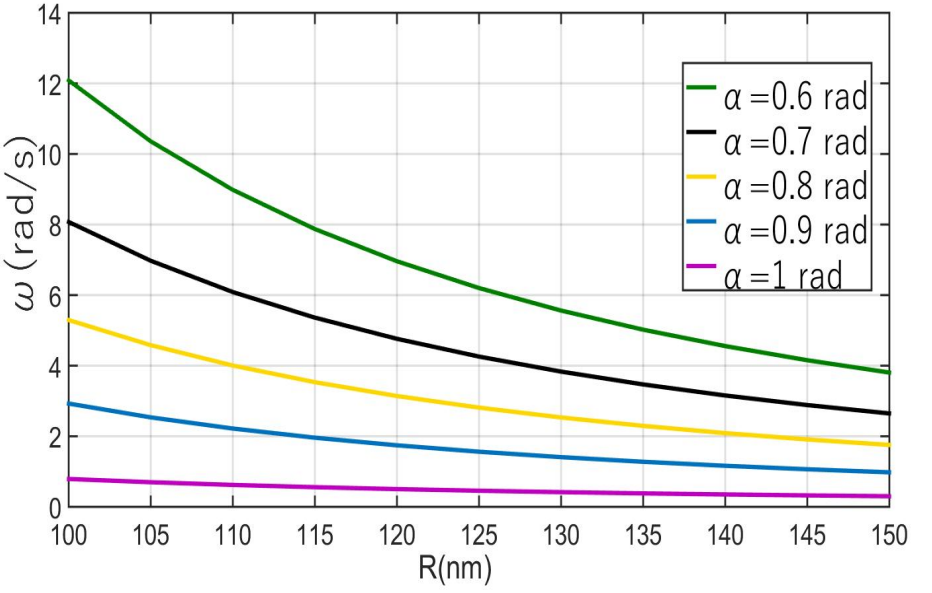

Figure 5.2.4. Natural frequency for different materials.

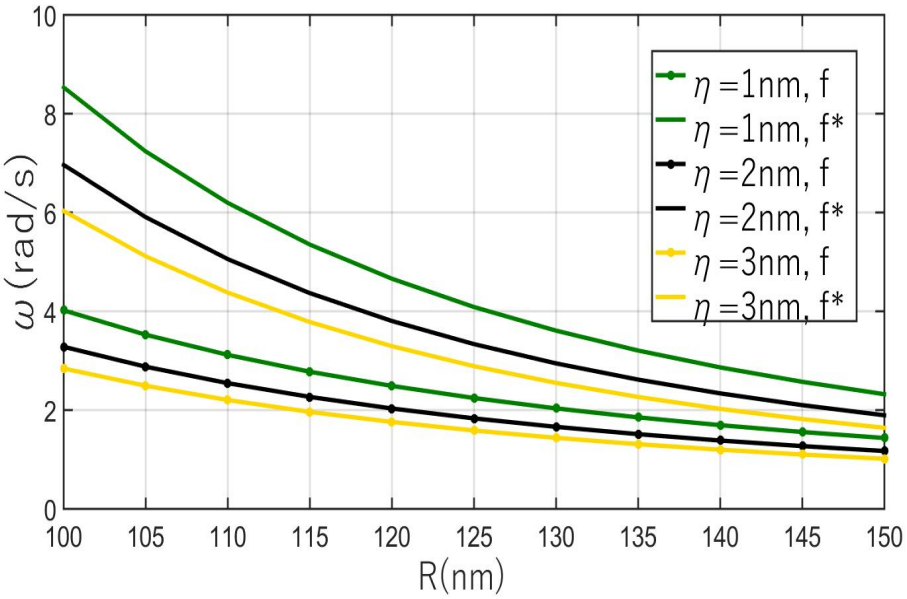

Figure 5.2.5. Natural frequency for two different shape functions.

5.2.1 Comparison and validation of the results

Table 5.2.1. The natural frequencies of clamped nanoarches for varying η.

		$\beta = 0.5\ rad$		$\beta = 2\ rad$	
Mode	η (nm)	Present	Ganapathi et al. [50]	Present	Ganapathi et al. [50]
1	0	24.8743	22.9609	36.2637	34.3728
	1	22.5673	21.5441	33.9981	31.9336
	2	21.4502	20.3559	31.9238	29.8975
	3	20.9901	19.3416	29.1047	28.1704
	4	20.0198	18.4629	28.9830	26.6855
2	0	54.6534	52.4678	45.5639	43.0525
	1	47.8765	45.5521	40.0184	37.8919
	2	41.9128	39.7231	36.7423	33.9014
	3	36.2049	35.5746	33.5642	30.8385
	4	32.7549	32.4808	31.9243	28.4340

Table 5.2.2. The natural frequencies of S-S and C-C nanoarches.

		$\beta = 1$ *rad*		$\beta = 2$ *rad*	
Mode	η (nm)	S-S	C-C	S-S	C-C
1	0	6.29953	6.36272	10.02100	10.35446
	1	4.47050	4.49912	7.05105	7.32999
	2	3.65442	3.67337	5.64782	5.98654
	3	3.16666	3.38114	4.46585	5.18510
	4	2.83332	2.86525	3.49793	4.63799
2	0	17.56912	17.85480	30.54324	31.11017
	1	15.45783	15.86733	21.54620	22.03271
	2	14.13590	14.75724	16.54670	17.99647
	3	13.99210	14.42905	14.75707	15.58794
	4	12.33064	13.63394	12.54678	13.94352

Chapter 6

Analysis of natural vibrations of cantilever nanoarches

This chapter discusses the results of the analysis of natural frequencies of cantilever nanoarches. The boundary conditions are

$$\begin{aligned} w(0) &= 0 \\ w^{'}(0) &= 0 \\ L_1 w(\beta) &= L_2 w^{''}(\beta) \\ L_1 w^{'}(\beta) &= L_2 w^{'''}(\beta), \end{aligned} \tag{6.0.1}$$

where
$L_1 = -\frac{EI-\rho h_1 \eta R^4 \omega^2}{R^2 \cdot (1+\eta)}$ and $L_2 = \frac{EI}{R^2(1+\eta)}$.

Here the general solution together with intermediate conditions is used in order to get numerical results. We get a system of five linear algebraic equations with five unknowns whose coefficients can be written in the form of a matrix. The system of equations has a non-trivial solution if and only if its determinant $\triangle$ equals zero. The determinant is

$$\triangle = \begin{vmatrix} K_{11} & K_{12} & K_{13} & K_{14} & K_{15} \\ K_{21} & K_{22} & K_{23} & K_{24} & K_{25} \\ K_{31} & K_{32} & K_{33} & K_{34} & K_{35} \\ K_{41} & K_{42} & K_{43} & K_{44} & K_{45} \\ K_{51} & K_{52} & K_{53} & K_{54} & K_{55} \end{vmatrix},$$

where

$$K_{11} = 0$$
$$K_{12} = 0$$
$$K_{13} = (L_1 - L_2\mu_1^2)(\nu_1 \cosh(\mu_1\beta)\cot(\nu_1\beta) - \mu_1 \sinh(\mu_1\beta))$$
$$K_{14} = (L_1 - L_2\mu_1^2)(\nu_1 \sinh(\mu_1\beta)\cot(\nu_1\beta) - \mu_1 \cosh(\mu_1\beta))$$
$$K_{15} = (L_1 + L_2\nu_1^2)(\nu_1 \cos(\nu_1\beta)\cot(\nu_1\beta) + \nu_1 \sin(\nu_1\beta))$$
$$K_{21} = -\cos(\nu_0\alpha) + \cosh(\mu_0\alpha)$$
$$K_{22} = \frac{\nu_0}{\mu_0}\sinh(\mu_0\alpha) - \sin(\nu_0\alpha)$$
$$K_{23} = \cosh(\mu_1\alpha) + \left(\frac{L_1 - L_2\mu_1^2}{L_1 + L_2\nu_1^2}\right)\left(\frac{\cosh(\mu_1\beta)}{\sin(\nu_1\beta)}\right)\sin(\nu_1\alpha)$$
$$K_{24} = \sinh(\mu_1\alpha) + \left(\frac{L_1 - L_2\mu_1^2}{L_1 + L_2\nu_1^2}\right)\left(\frac{\sinh(\mu_1\beta)}{\sin(\nu_1\beta)}\right)\sin(\nu_1\alpha)$$
$$K_{25} = \cos(\nu_1\alpha) + \left(\frac{\cos(\nu_1\beta)}{\sin(\nu_1\beta)}\right)\sin(\nu_1\alpha)$$

$$
\begin{aligned}
K_{31} &= p\nu_0^2\cos(\nu_0\alpha) + p\mu_0^2\cosh(\mu_0\alpha) \\
&\quad + \nu_0\sin(\nu_0\alpha) - \mu_0\sinh(\mu_0\alpha) \\
&\quad - p\cos(\nu_0\alpha) + p\cosh(\mu_0\alpha) \\
K_{32} &= \nu_0^2\sin(\nu_0\alpha) + p\mu_0\nu_0\sinh(\mu_0\alpha) \\
&\quad - p\sin(\nu_0\alpha) + p\left(\frac{\nu_0}{\mu_0}\right)\sinh(\mu_0\alpha) \\
&\quad - \nu_0\cos(\nu_0\alpha) \\
K_{33} &= u_1\sinh(u_1\alpha) + \left(\frac{L_1 - L_2u_1^2}{L_1 + L_2\nu_1^2}\right)\left(\frac{\cosh(u_1\beta)}{\sin(\nu_1\beta)}\right)\nu_1\cos(\nu_1\alpha) \\
K_{34} &= u_1\cosh(u_1\alpha) + \left(\frac{L_1 - L_2u_1^2}{L_1 + L_2\nu_1^2}\right)\left(\frac{\sinh(u_1\beta)}{\sin(\nu_1\beta)}\right)\nu_1\cos(\nu_1\alpha) \\
K_{35} &= \nu_1\cot(\nu_1\beta)\cos(\nu_1\alpha) - \nu_1\sin(\nu_1\alpha)
\end{aligned}
$$

$$
\begin{aligned}
K_{41} &= \nu_0^2\cos(\nu_0\alpha) - \mu_0^2\cosh(\mu_0\alpha) \\
K_{42} &= \nu_0^2\sin(\nu_0\alpha) - \nu_0\mu_0\sinh(\mu_0\alpha) \\
K_{43} &= \mu_1^2\cosh(\mu_1\alpha) + \left(\frac{L_1 - L_2\mu_1^2}{L_1 + L_2\nu_1^2}\right)\left(\frac{\cosh(\mu_1\beta)}{\sin(\nu_1\beta)}\right)\nu_1^2\sin(\nu_1\alpha) \\
K_{44} &= \mu_1^2\sinh(\mu_1\alpha) + \left(\frac{L_1 - L_2\mu_1^2}{L_1 + L_2\nu_1^2}\right)\left(\frac{\sinh(\mu_1\beta)}{\sin(\nu_1\beta)}\right)\nu_1^2\sin(\nu_1\alpha) \\
K_{45} &= \nu_1^2\cot(\nu_1\beta)\sin(\nu_1\alpha) - \nu_1^2\cos(\nu_1\alpha)
\end{aligned}
$$

$$K_{51} = -\nu_0^3 \sin(\alpha\beta) + \mu_0^3 \sinh(\mu_0\alpha)$$
$$K_{52} = \nu_0^3 \cos(\alpha\beta) + \nu_0\mu_0^2 \cosh(\mu_0\alpha)$$
$$K_{53} = \mu_1^3 \sinh(\mu_1\alpha) - \left(\frac{L_1 - L_2\mu_1^2}{L_1 + L_2\nu_1^2}\right)\left(\frac{\cosh(\mu_1\beta)}{\sin(\nu_1\beta)}\right)\nu_1^3 \cos(\nu_1\alpha)$$
$$K_{54} = \mu_1^3 \cosh(\mu_1\alpha) + \left(\frac{L_1 - L_2\mu_1^2}{L_1 + L_2\nu_1^2}\right)\left(\frac{\sinh(\mu_1\beta)}{\sin(\nu_1\beta)}\right)\nu_1^3 \cos(\nu_1\alpha)$$
$$K_{55} = \nu_1^3 \cot(\nu_1\beta)\cos(\nu_1\alpha) + \nu_1^3 \sin(\nu_1\alpha).$$

6.1 Results and discussion

Numerical results are obtained for a specimen made of a nanomaterial with the modulus of elasticity $E = 7 \times 10^{11}\ Pa$, $\nu = 0.3$, $\rho = 10\ kg/m^3$. The radius of the middle line of the arch $R = 110\ nm$ and the width $b = 1\ nm$ if the text does not contain any numerical evaluations of these quantities. The natural frequencies for the first mode are presented in Figures 6.1.1-6.1.12 and Tables 6.1.1 and 6.1.2. In Figures 6.1.1-6.1.3, the natural frequency of the nanoarch is depicted versus the thickness of the nanoarch for different values of the radius. Here $R = 80 - 120\ nm$ and Figures 6.1.1-6.1.3 correspond to $\alpha = 0.8, 0.6$ and $0.4\ rad$, respectively. Looking at the figures, one can draw a conclusion that the smaller is the radius, the higher is the natural frequency of the nanoarch for given value of the thickness. Also, one can see from the figures that thicker nanoarches have higher natural frequencies, provided the radius R is fixed. The figures reveal another noteworthy conclusion: as the value of α increases, the impact of the thickness on the natural frequency of the nanoarches becomes greater. Three different curves depicting the relationship between natural frequencies and crack length are presented in Figures 6.1.4-6.1.6, each curve corresponding to a different value of the nonlocal parameter η. Specifically, Figures 6.1.4-6.1.6 correspond to the values of $\alpha = 0.8, 0.6, 0.4\ rad$, respectively. The figures indicate

that the natural frequency decreases as the crack length increases. Notably, a significant decrease in frequency occurs when the crack length surpasses 0.5. Additionally, the figures reveal that lower values of alpha are associated with decreased natural frequencies.

Figure 6.1.7 illustrates the relationship between the natural frequency of the nanoarch and the nonlocal parameter. The curves on the graph correspond to different values of the radius. It is evident from the figure that as the nonlocal parameter η increases, the frequency of the nanoarch decreases. This behaviour is also observed when examining the natural frequency concerning the radius. The relationship between the natural frequency and the location of the defect is depicted in Figure 6.1.8. Each curve on the graph corresponds to a different crack length. It is noticeable from the figure that initially, the natural frequency decreases, but then it begins to increase. Once the crack location exceeds 0.5 *rad*, the natural frequency experiences a significant increase. The effects of varying crack lengths can also be seen in the figure.

In Figure 6.1.9, the natural frequency is plotted against the radius of the nanoarch. Different curves in the figure correspond to the various positions of the defect. It can be seen in the figure that the natural frequency decreases with an increase of the radius. However, the influence of the radius on natural frequency is less observable for higher values of alpha. Figure 6.1.10 illustrates the relationship between the natural frequency of the nanoarches and their thickness. Here the thickness of the nanoarch is varying between 0 and α. The figure clearly shows that as the thickness of the nanoarch increases, so does the natural frequency. Different curves in Figure 6.1.10 represent various values of the radius, revealing the matter that the frequency decreases as the radius of the arch increases.

Figure 6.1.11 shows the relationship between the natural frequency and the central angle β of the nanoarch. Different curves in Figure 6.1.11 correspond to different values of the nonlocal parameter η. It can be seen from Figure 6.1.11 that the natural frequency is higher for larger values of the central angle β. On the other hand, the smaller is the nonlocal parameter η the higher is the natural frequency. In Figure 6.1.12, the natural frequency is depicted against the radius of the nanoarch, show-

casing the influence of various shape functions. From the figure, it is evident that the choice of shape functions significantly impacts the natural frequency of the arches.

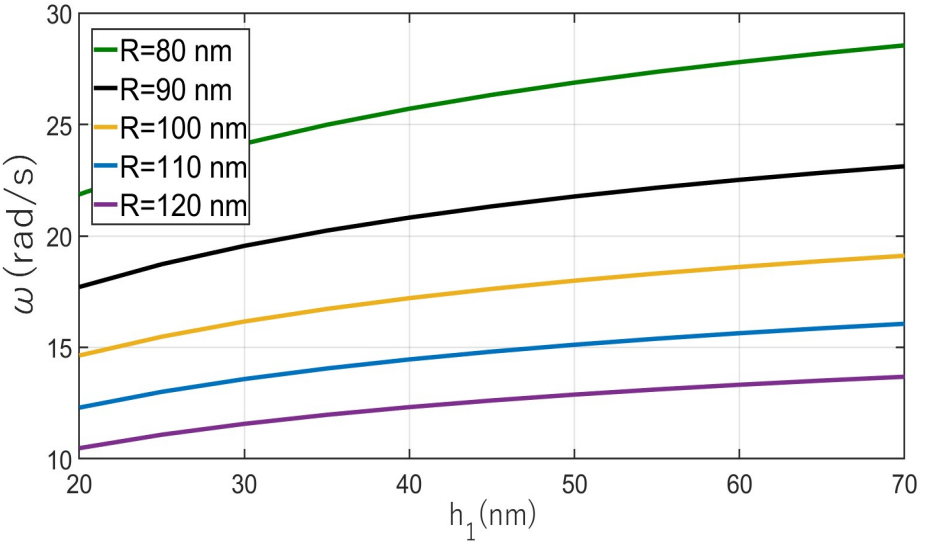

Figure 6.1.1. Natural frequency versus thickness for $\alpha = 0.8\ rad$.

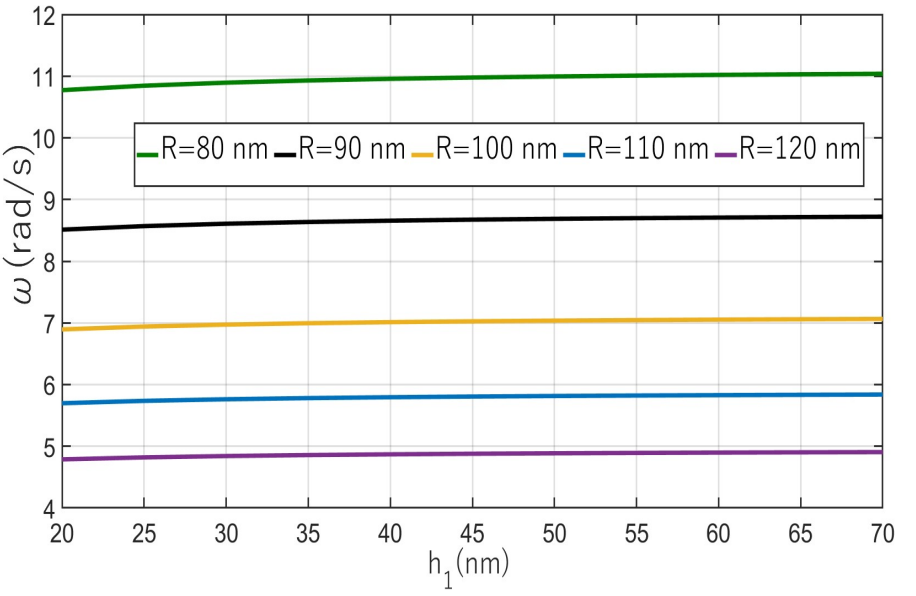

Figure 6.1.2. Natural frequency versus thickness for $\alpha = 0.6\ rad$.

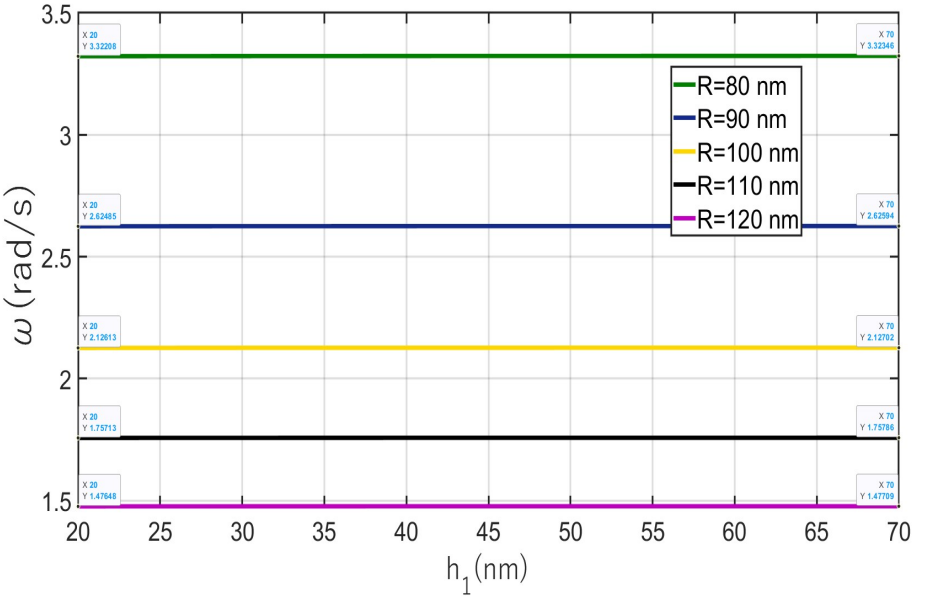

Figure 6.1.3. Natural frequency versus thickness for $\alpha = 0.4\ rad$.

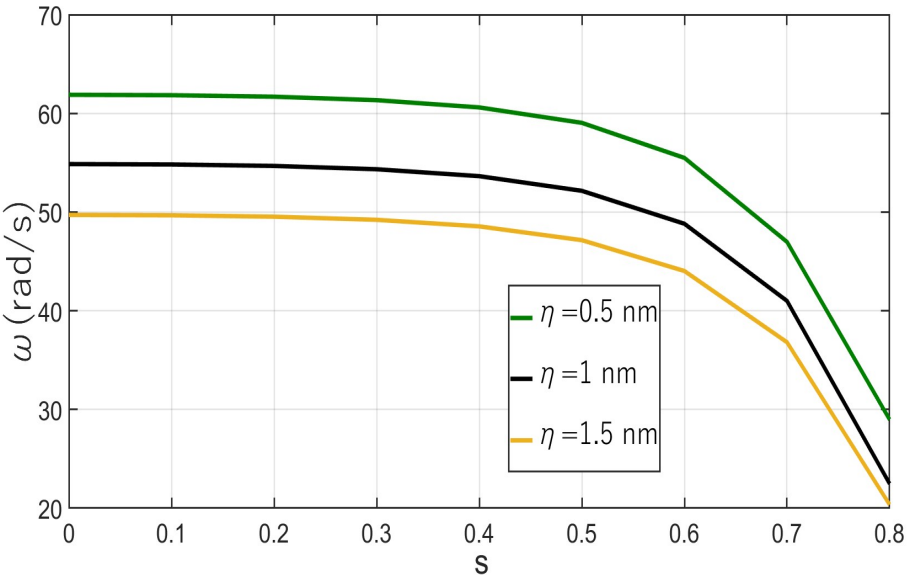

Figure 6.1.4. Natural frequency versus crack length for $\alpha = 0.8$ *rad*.

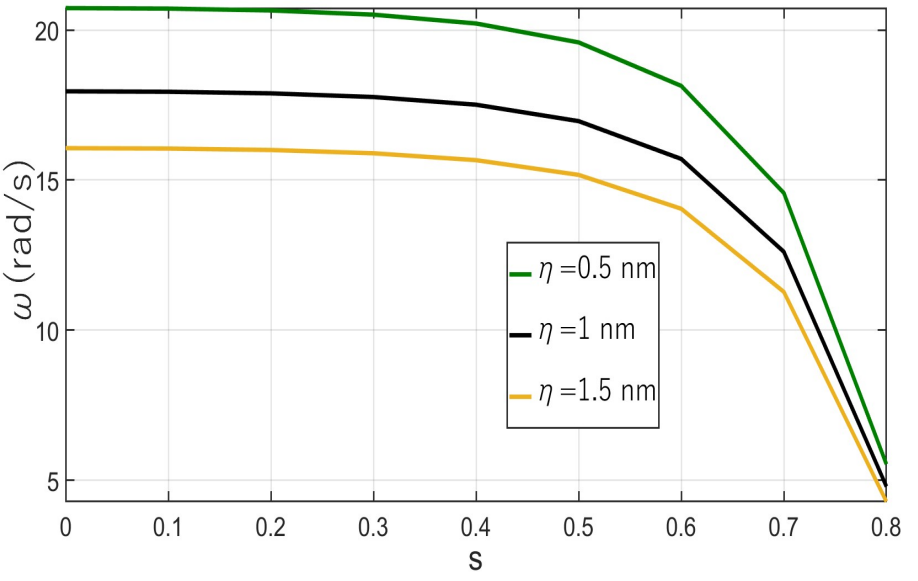

Figure 6.1.5. Natural frequency versus crack length for $\alpha = 0.6$ *rad*.

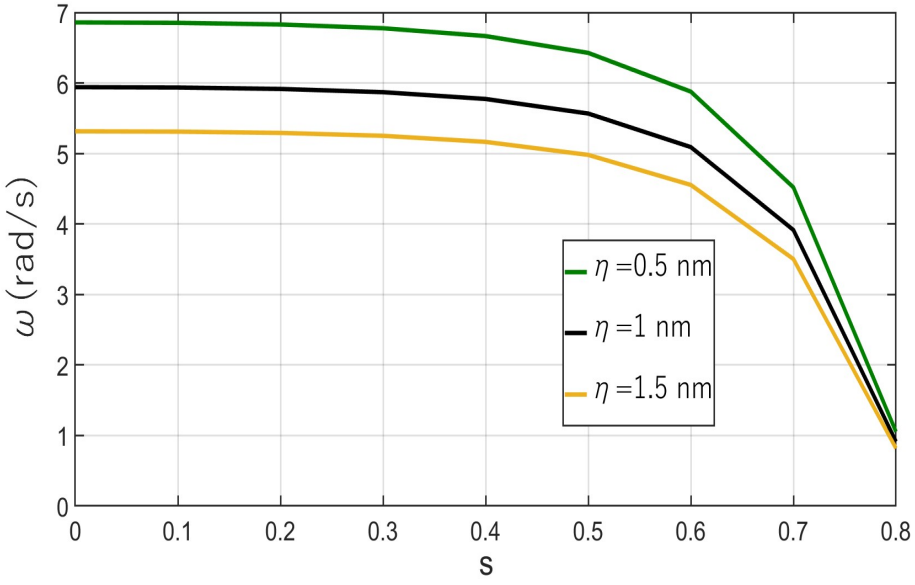

Figure 6.1.6. Natural frequency versus crack length for $\alpha = 0.4$ *rad*.

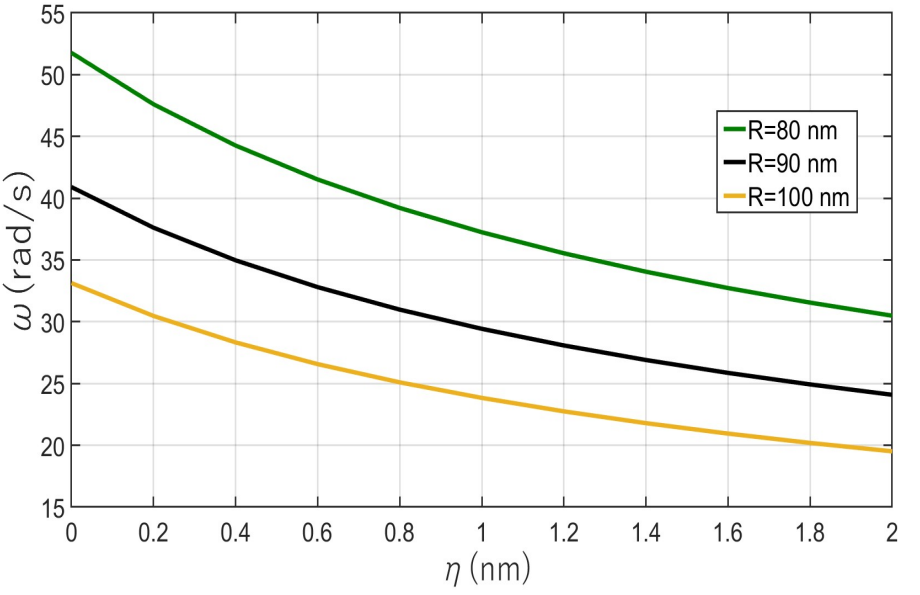

Figure 6.1.7. Natural frequency versus nonlocal parameter.

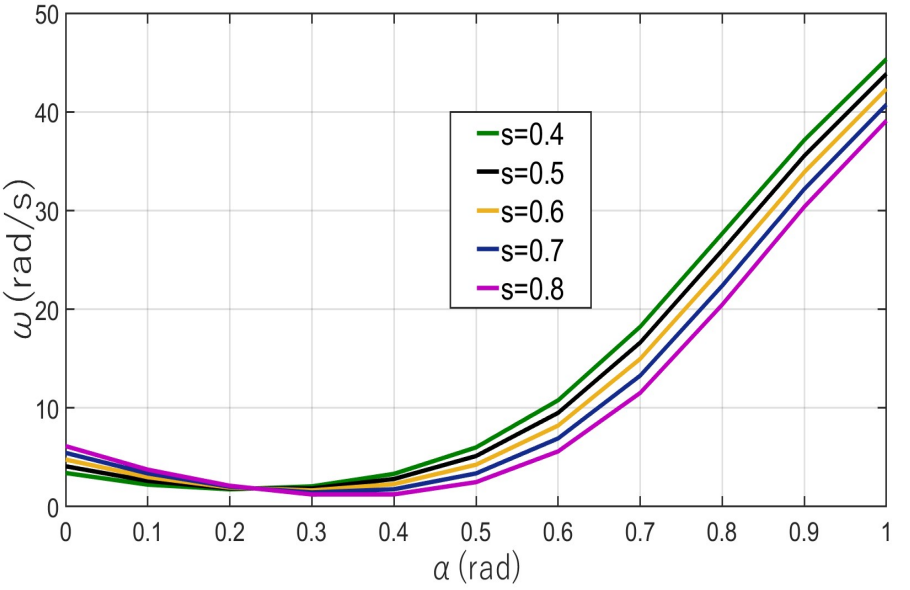

Figure 6.1.8. Natural frequency versus defect location.

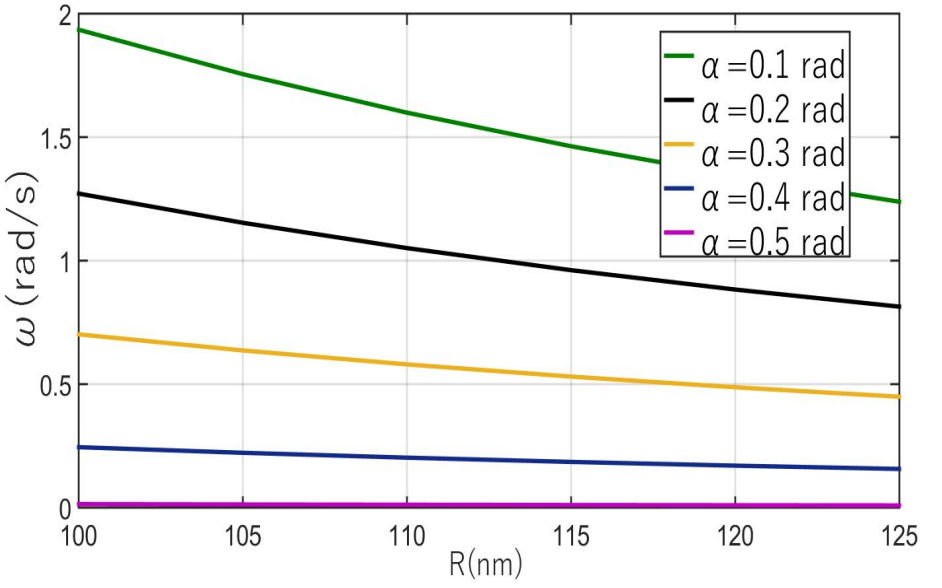

Figure 6.1.9. Natural frequency versus radius of the nanoarch.

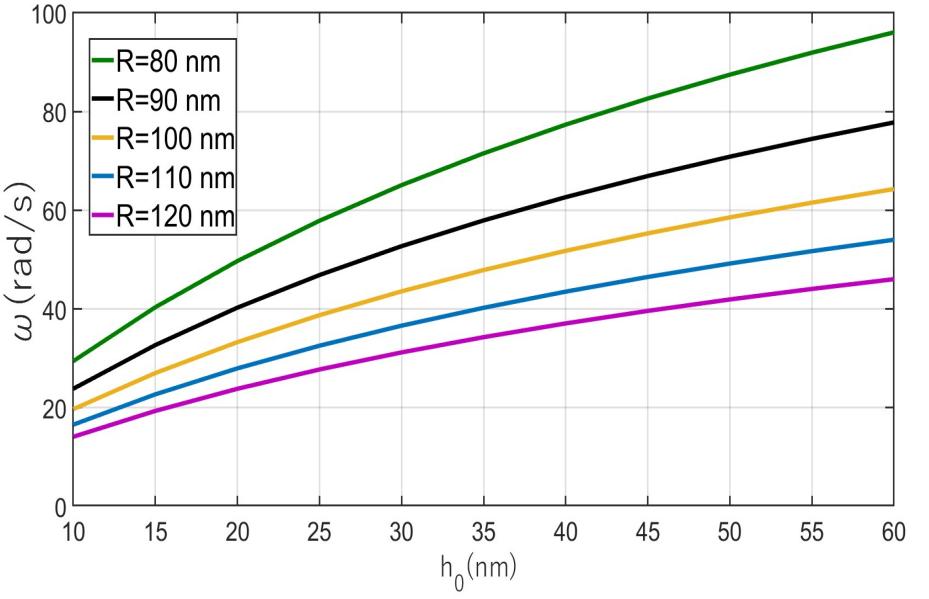

Figure 6.1.10. Natural frequency versus thickness h_0 of the nanoarch.

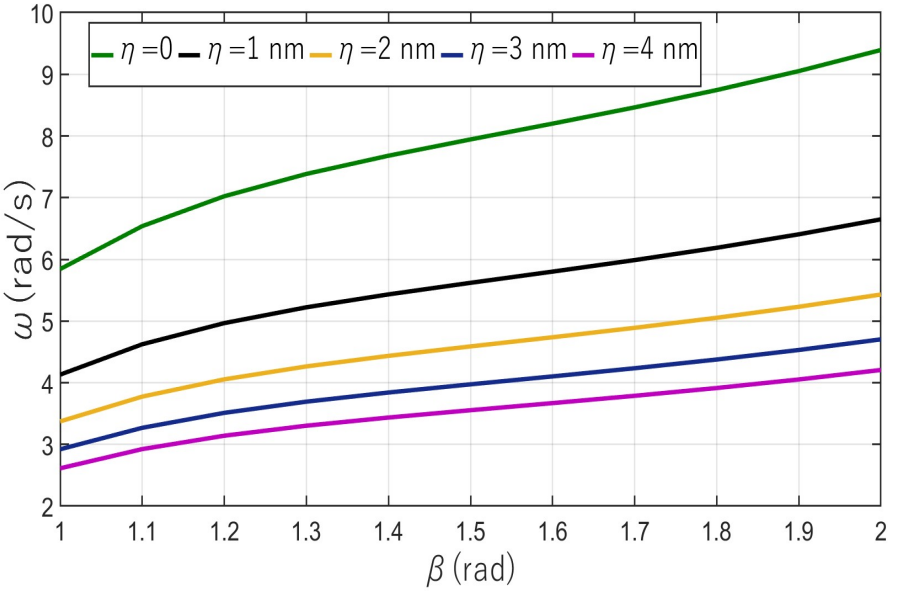

Figure 6.1.11. Natural frequency versus central angle of the nanoarch.

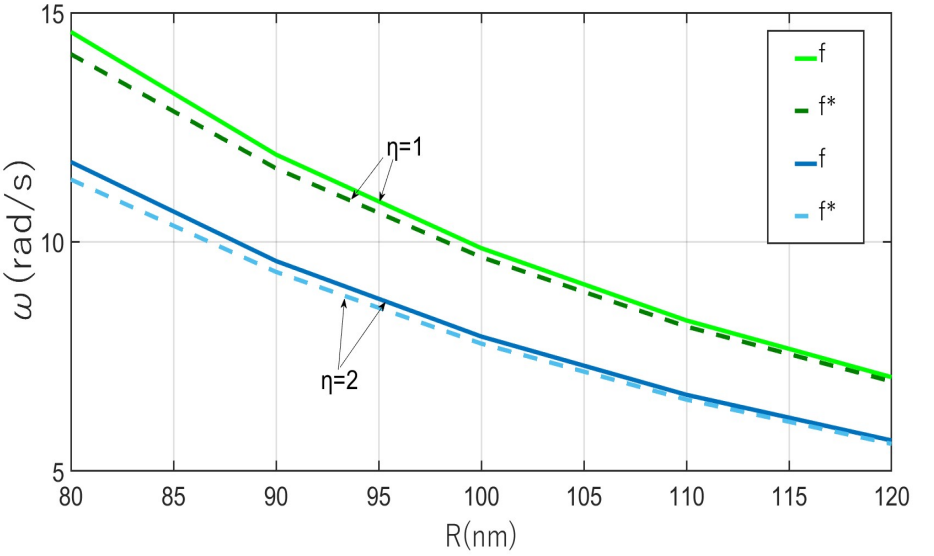

Figure 6.1.12. Natural frequency versus radius of the nanoarch for different shape functions.

6.1.1 Comparison of the results

Natural frequencies of nanoarches clamped at the left edge and free at the right-hand edge are presented in Table 6.1.1. Table 6.1.1 corresponds to the arches with $\beta = 0.5\ rad$. Table 6.1.2 accommodates corresponding values of the natural frequency for arches fully clamped at both edges for different values of the parameter η (here $0 \leq \eta \leq 4$). In Table 6.1.1, the results of the current work are compared with those obtained by Ganapathi et al. [50], making use of the finite element method. The comparison of the eigenfrequencies found by different methods shows that the current method leads to somewhat overestimated values of natural frequencies. That is why the eigenfrequencies calculated by the current method are higher than those corresponding to Ganapathi et al. [50]. The present calculation method is also applied to full nanorings ($\beta = 2\pi\ rad$). The obtained results of calculations are accommodated together with the results by Wang and Duan [141] in Table 6.1.2 for different values of the nonlocal parameter η. It can be seen from Table 6.1.2 that the results

obtained by the current method are close to those obtained by Wang and Duan. Despite our results are higher than those found in [50], these are lower than the results of Wang and Duan [141]. Table 6.1.3 compares natural frequencies of S-S, C-F and C-C nanoarches for the first and second modes.

Table 6.1.1. Comparison of the current results with Ganapathi et al. [50]

	$\beta = 0.5\ rad$		
Mode	η (nm)	Present	Ganapathi et al.[50]
1	0	5.1132	3.5078
	1	4.8045	3.4289
	2	4.5771	3.3546
	3	4.1808	3.2847
	4	3.8474	3.2187
2	0	21.6534	19.8974
	1	18.9765	17.6058
	2	17.0128	15.9352
	3	15.2049	14.6692
	4	14.7549	13.6734

Table 6.1.2. Natural frequency of circular nanorings.

	$a = 0.2$		$a = 0.4$	
Mode	Present	Wang and Duan [141]	Present	Wang and Duan [141]
1	5.6234	6.2	3.2089	4.4
2	41.2437	42.4	21.8362	23.6
3	127.2065	129.1	57.5028	59.5
4	274.3769	276.9	107.7692	110.8
5	485.1752	488.5	173.1745	176.3
		Nanoring with a defect		
1	4.9908	5.9	3.2543	4.2
2	39.1549	40.8	21.8654	23.1
3	123.7280	125.0	56.5437	58.6
4	267.8756	270.0	107.0654	109.6
5	475.5538	478.6	172.1767	174.9

Table 6.1.3. The natural frequencies of S-S, C-F and C-C nanoarches.

		$\beta = 1$ *rad*			$\beta = 2$ *rad*		
Mode	η (nm)	S-S	C-F	C-C	S-S	C-F	C-C
1	0	6.2995	6,3265	6.3627	10.0210	10.1418	10.3544
	1	4.4705	4.4830	4.4991	7.0510	7.1902	7.3299
	2	3.6544	3.2488	3.6733	5.6478	5.7213	5.9865
	3	3.1666	3.6621	3.3811	4.4658	4.8310	5.1851
	4	2.8333	3.2001	2.8652	3.4979	3.8316	4.6379
2	0	17.5692	17.7321	17.8548	30.5432	30.8821	31.1101
	1	15.4578	15.6313	15.8673	21.5462	21.7218	22.0327
	2	14.1359	14.4031	14.7572	16.5467	17.2111	17.9964
	3	13.9921	14.1938	14.4290	14.7570	14.9901	15.5879
	4	12.3306	13.2014	13.6339	12.5467	12.7189	13.9435

Chapter 7

Nonlocal theory of elasticity in the natural vibrations of the CNTs

7.1 Carbon nanotubes

7.1.1 Introduction

Coal and diamond, sand, computer chips, cancer and healthy tissues all have one thing in common: variations in the arrangement of atoms. Depending on how the atoms are arranged, they can form elements as diverse as soil, air, water, or even delicious ripe strawberries. Our ability to manipulate the arrangement of atoms lies at the very foundation of nanotechnology. In 1991, Sumio Iijma made a groundbreaking discovery when he found carbon nanotubes (CNTs). The term "nano" refers to a unit of length scale, equivalent to 10^{-9} meters, which is hundreds to thousands of times smaller than a typical biological cell or bacterium. CNTs possess a unique molecular structure and exhibit fascinating mechanical and electrical properties, making them versatile and applicable in various fields. Due to their distinctive characteristics, CNTs find application in multiple technologies and industries, taking advantage of

their exceptional mechanical strength and impressive electrical conductivity. These qualities have opened up new avenues in nanotechnology, paving the way for innovative materials and devices with remarkable properties. Therefore, it is imperative to understand the structure before we study the static and dynamic behaviour of CNTs.

7.1.2 Structure and types of the CNTs

The structure of CNTs is fascinating and can be formed as a result of the folding of one or more layers of graphite, forming a cylindrical shape composed of interconnected carbon hexagons. Each end of the cylinder exhibits a hemispherical "cap", as depicted in Figure 7.1.1. One of the critical features of CNTs is that they are entirely composed of sp^2 bonds, which are more robust than the sp^3 bonds typically found in diamonds. This unique bonding structure grants them exceptional strength, making them remarkably strong at the nanoscale. Additionally, nanotubes tend to align themselves into rope-like structures held together by Van der Waals forces. This arrangement enables the formation of nanotube ropes, providing further strength and structural integrity to the material. Interestingly, nanotubes can merge and bond under high pressure, trading some sp^2 bonds for sp^3 bonds. This behaviour opens exciting possibilities for producing strong, unlimited-length wires through high-pressure nanotube linking.

Basically, nanotubes are divided into two types depending on the layers of the graphene sheet; Single-walled carbon nanotubes (SWCNTs) and Multi-walled carbon nanotubes (MWCNTs). The geometrical structures of SWCNTs are specified by a pair of chiral indices (n, m). These indices determine the orientation of the graphene lattice concerning the tube axis, resulting in three distinct types: armchair (n, n), zigzag (n, 0) and chiral (n, m) [104].

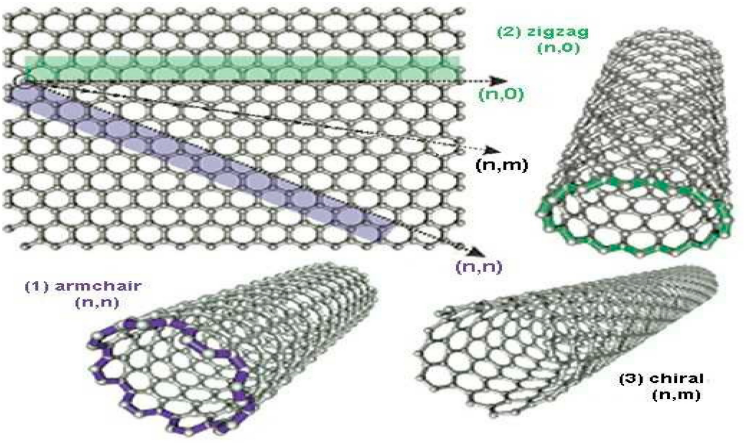

Figure 7.1.1. SWCNTs by rolling a graphene sheet in different directions [104].

7.1.3 Applications of the CNTs

- CNTs exhibit unique electronic and mechanical properties because of their increased surface area-to-volume ratio. Several applications of CNTs in different fields of engineering have been discovered. Some of the applications discussed by Ajayan et al. [5] are as follows:

- Carbon nanotubes, because of nanometer-size diameter, structural integrity, high electrical conductivity and chemical stability, are good electron emitters.

- Nanotubes can be used as reinforcements in composite materials because CNTs will increase the toughness of the composites by absorbing energy during highly flexible elastic experiences.

- Nanotube-filled polymers can be used in applications of electromagnetic induction shielding.

- Because of their hollow geometry and nano-scale diameter, it has been predicted that carbon nanotubes can store liquid and gas in the inner cores through a capillary effect.

- Due to nanosize, high conductivity, high mechanical strength and flexibility, CNTs are used in electrical and other scanning probe instruments, such as an electrostatic force microscope.
- CNTs tips are used in a tapping mode to image biological molecules such as amyloid-protofibrils with a resolution never achieved before.
- CNTs have relatively straight and narrow channels in their cores, which can be filled with foreign materials to fabricate one-dimensional nanowires.

7.2 Natural vibrations of SWCNTs

7.2.1 Formulation and solution of the problem

CNTs are cylindrical nanostructures and when they are bent or curved, they exhibit properties similar to those of curved nanobeams. In this context, a carbon nanotube with a curved shape can be considered a curved nanobeam due to its slender, elongated structure with a curved geometry. Vibrations of CNTs are studied by using a beam model by Behera and Chakraverty [22].
Here we consider a curved CNT with simply supported boundary conditions. We also assume that the CNT is damaged with a crack-like defect. To set up the governing equations for the natural vibrations of simply supported CNTs, the problem is formulated as in Section (3.1).

7.2.2 Results and discussion

Natural frequencies for the first mode are presented for the SWCNTs of different types with simply supported edges. Physical properties of the CNTs are taken from published literature [56] and [98]. Here the values $\beta = 1\ rad$, $\eta = 1\ nm$ and crack length $s = 0.4$ are considered where values of these parameters are not specified in the legends. In Figure 7.2.1, the natural frequency of the CNTs is plotted against the central angle β. From the figure, one can observe that the natural frequency initially

increases and then starts decreasing as we increase the β value. It is also noticeable that the frequency for the chiral nanotubes is higher than that of armchair and zigzag nanotubes. Figure 7.2.2 shows the natural frequency plotted against the nonlocal parameter η. The figure illustrates the matter that the frequency consistently decreases as we increase the η. Furthermore, it can be seen that the zigzag nanotubes exhibit the lowest frequency compared to other nanotubes. In Figure 7.2.3, the natural frequency is plotted against the radius of the CNTs. It is clear from the figure that the frequency decreases as the value of the radius increases. Figures 7.2.3-7.2.5 depict the natural frequencies of armchair, zigzag, and chiral CNTs, plotted against the radius of nanotubes. Different curves in the figures correspond to different values of η.

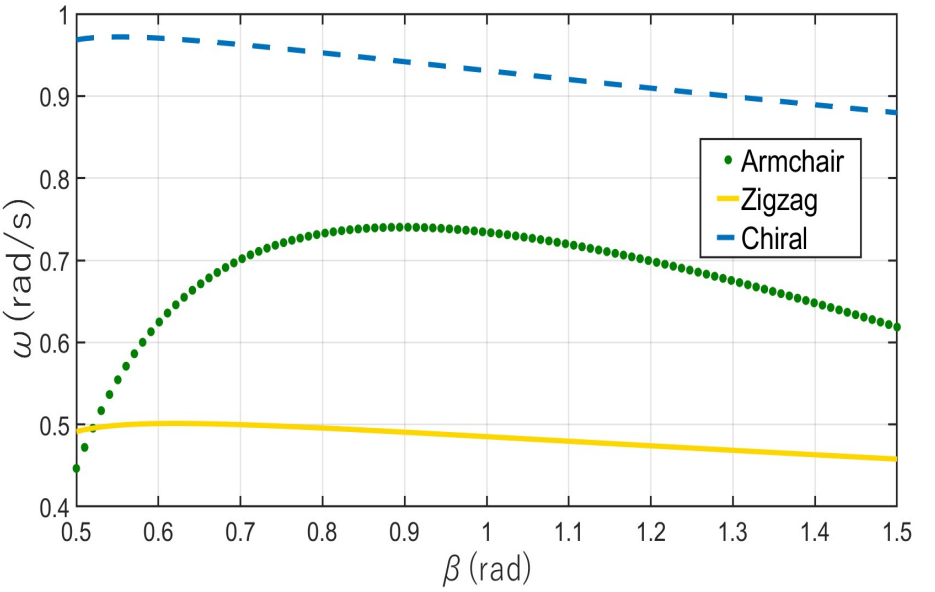

Figure 7.2.1. Natural frequency versus central angle of the CNTs.

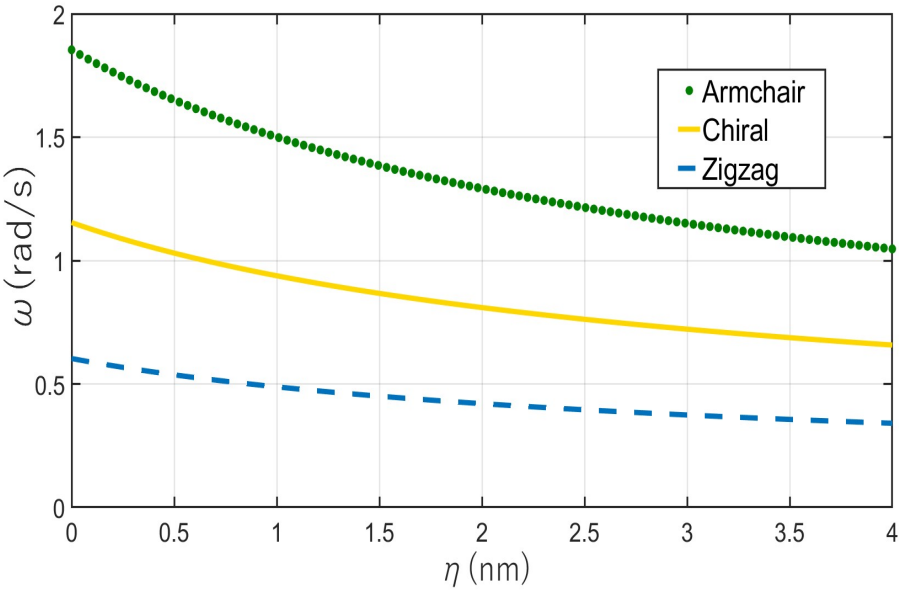

Figure 7.2.2. Natural frequency versus the nonlocal parameter.

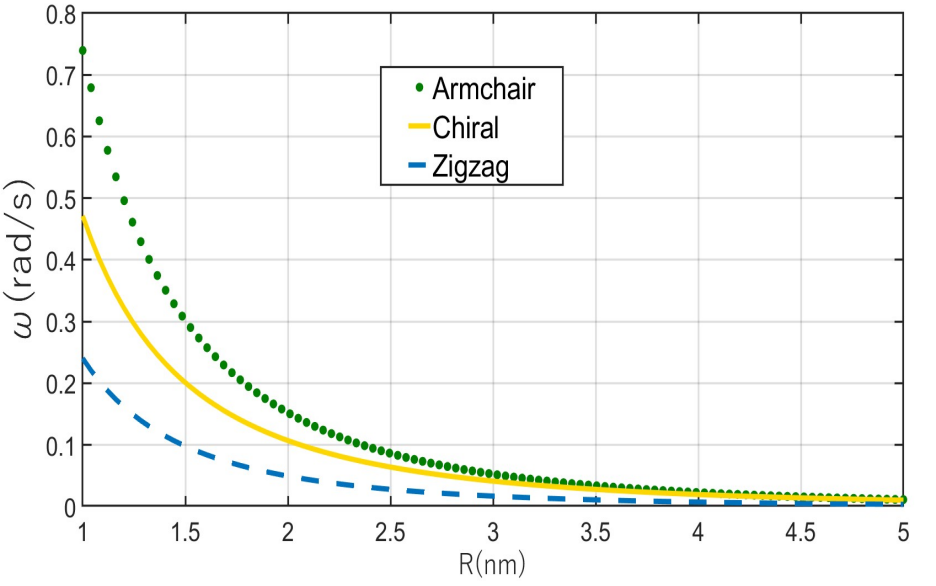

Figure 7.2.3. Natural frequency versus radius of the CNTs.

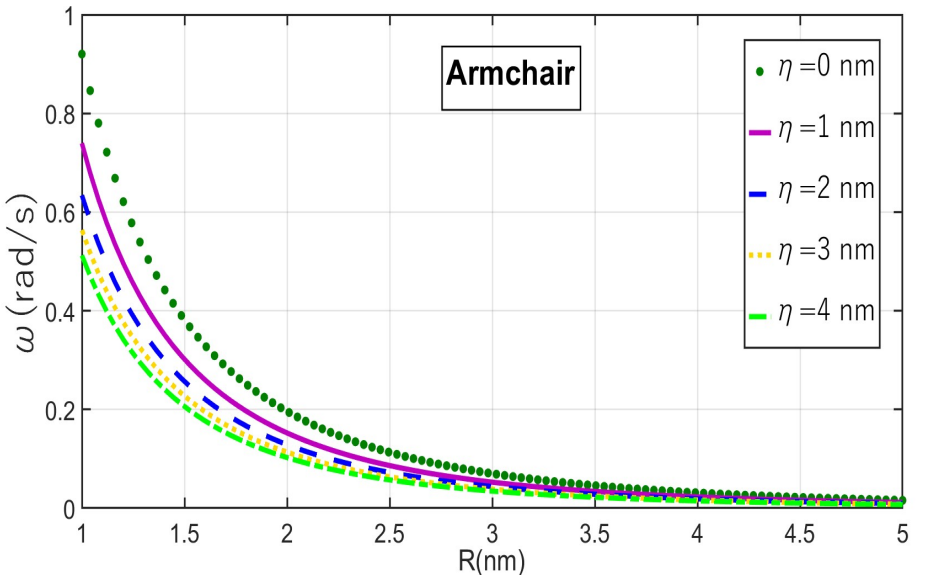

Figure 7.2.4. Natural frequency versus radius of the armchair CNT.

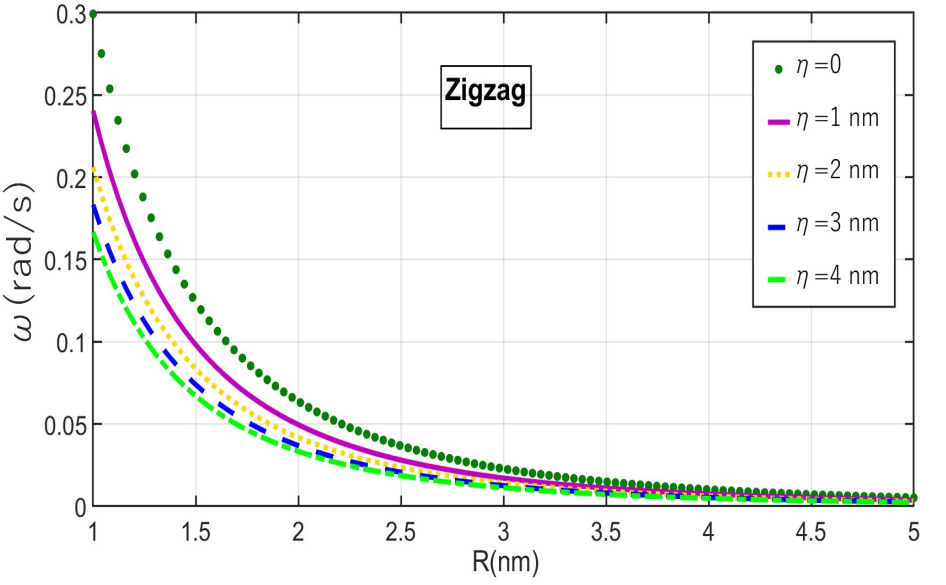

Figure 7.2.5. Natural frequency versus radius of the zigzag CNT.

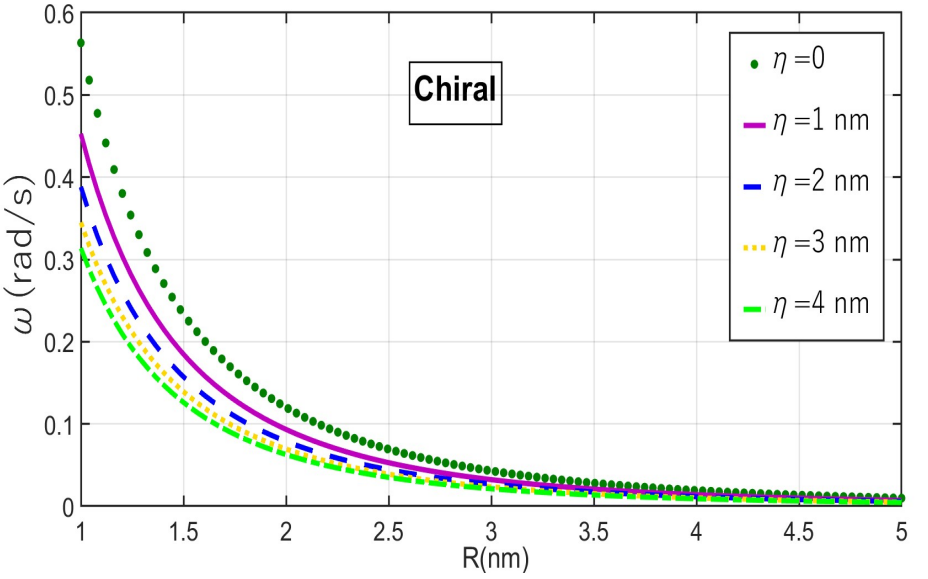

Figure 7.2.6. Natural frequency versus radius of the chiral CNT.

Table 7.2.1. Material properties of carbon nanotubes.

Physical properties	Armchair $(10,10)$	Zigzag $(10,0)$	Chiral $(10,2)$
Radius (R)	0.6427 nm	0.3713 nm	0.4134 nm
Wall thickness (h)	0.1232 nm	0.0878 nm	0.0974 nm
Density (ρ)	1.33 g/cm^3	2.3 g/cm^3	1.40 g/cm^3
Poisson ratio (v)	0.180	0.265	0.209
Young's modulus (E)	2.618 TPa	3.939 TPa	3.456 TPa

Concluding remarks

The current study focuses on investigating the natural vibrations of curved nanobeams. The nonlocal theory of elasticity is employed to calculate the natural frequency of nanoarches, as the classical theory fails in considering small-length scale effects. Specifically, the study examines the impact of crack-like defects on the natural frequency of the nanoarches and compares the results.

In addition, the study considers nanoarches with piecewise constant thickness, where stable cracks are located at the re-entrant corners of steps. A novel method based on linear elastic fracture mechanics is developed to determine the natural frequencies. Through the calculations, it becomes evident that the presence of cracks significantly affects the natural frequency. Notably, nanoarches without any defects exhibit the lowest natural frequencies. Furthermore, the study explores how the steps in the nanoarches influence their vibrational behaviour. The results are compared with those reported by other researchers, demonstrating favourable agreement, particularly for small values of the nonlocal parameter.

Both, simply supported and clamped nanoarches are studied. It is discovered that clamped nanoarches exhibit higher natural frequencies than simply supported nanoarches. Additionally, the natural frequency of cantilever nanoarches with cracks and steps is calculated. The results are compared with those available in the literature. The study also indicates that the natural frequency of cantilever nanoarches falls between the frequencies of simply supported and clamped nanoarches. The presence and the position of cracks significantly influence the frequency be-

haviour, with longer cracks leading to lower natural frequencies. The method to determine the natural frequency of the curved nanobeams is also applied to calculate the frequencies of the SWCNTs of the shapes armchair, zigzag and chiral.

The study employs the method of separation of the variables to get closed-form solutions of the governing equations. The obtained results are validated by comparing them with those in the existing literature. However, it is essential to highlight that cracks play a significant role in altering the frequency behaviour of curved beams.

Furthermore, the study extensively discusses the influence of various physical parameters such as thickness, radius and central angle of the nanoarches. Additionally, the study identifies that the position of the crack also affects the natural frequency; longer cracks lead to lower natural frequencies. Finally, this study emphasises the significance of cracks and steps in nanoarches and sheds light on the intricate relationship between these defects and the frequency behaviour of the arch. From the numerical results, it is concluded that

1. The natural frequency of the nanoarch with a step is higher than that of without the step.

2. Natural frequency decreases with the increase of the crack length in the case of the simply supported nanoarches but decreases in the case of clamped-free nanoarches.

3. Nonlocal parameters cause a decrease in the natural frequency of the nanoarches. This means that the frequencies calculated in classical theory are higher than those calculated by using the nonlocal theory of elasticity.

4. With the increase of central angle and thickness of the arches, natural frequency increases.

5. The natural frequency of the nanoarch depends on the position of the crack and on the extension of the crack.

Bibliography

[1] N. Abid, A. M. Khan, S. Shujait, K. Chaudhary, M. Ikram, M. Imran, J. Haider, M. Khan, Q. Khan, and M. Maqbool, *Synthesis of nanomaterials using various top-down and bottom-up approaches, influencing factors, advantages, and disadvantages: A review*, Adv. Colloid Interface Sci. **300** (2022), 102597.

[2] S. Adhikari, D. Karličić, and X. Liu, *Dynamic stiffness of nonlocal damped nano-beams on elastic foundation*, Eur. J. Mech. A-Solids **86** (2021), 104144.

[3] I. Ahmadi, *Vibration analysis of 2D-functionally graded nanobeams using the nonlocal theory and meshless method*, Eng. Anal. Bound. Elem. **124** (2021), 142–154.

[4] M. Ahmadvand and P. Asadi, *Free vibration analysis of flexible rectangular fluid tanks with a horizontal crack*, Appl. Math. Model. **91** (2021), 93–110.

[5] P. M. Ajayan, L. S. Schadler, and P. V. Braun, *Nanocomposite Science and Technology*, John Wiley & Sons, 2006.

[6] A. S. Y. Alsabbagh, O. M. Abuzeid, and M. H. Dado, *Simplified stress correction factor to study the dynamic behavior of a cracked beam*, Appl. Math. Model. **33** (2009), 127–139.

[7] T. L. Anderson, *Fracture Mechanics: Fundamentals and Applications*, CRC Press, 2005.

[8] N. Anifantis and A. Dimarogonas, *Stability of columns with a single crack subjected to follower and vertical loads*, Int. J. Solids Struct. **19** (1983), 281–291.

[9] R. Ansari, H. Rouhi, and S. Sahmani, *Calibration of the analytical nonlocal shell model for vibrations of double-walled carbon nanotubes with arbitrary boundary conditions using molecular dynamics*, Int. J. Mech. Sci. **53** (2011), 786–792.

[10] R. Ansari and S. Sahmani, *Bending behavior and buckling of nanobeams including surface stress effects corresponding to different beam theories*, Int. J. Eng. Sci. **49** (2011), 1244–1255.

[11] M. Arefi, E. M. Bidgoli, R. Dimitri, M. Bacciocchi, and F. Tornabene, *Nonlocal bending analysis of curved nanobeams reinforced by graphene nanoplatelets*, Compos. Part B Eng. **166** (2019), 1–12.

[12] M. Arefi and A. M. Zenkour, *Thermal stress and deformation analysis of a size-dependent curved nanobeam based on sinusoidal shear deformation theory*, Alex. Eng. J. **57** (2018), 2177–2185.

[13] A. I. Aria, M. I. Friswell, and T. Rabczuk, *Thermal vibration analysis of cracked nanobeams embedded in an elastic matrix using finite element analysis*, Compos. Struct. **212** (2019), 118–128.

[14] N. M. Auciello and De Rosa, *Free vibrations of circular arches: A review*, J. Sound Vib. **176** (1994), 433–458.

[15] W. J. Austin and A. S. Veletsos, *Free vibration of arches flexible in shear*, J. Eng. Mech. Div. **99** (1973), 735–753.

[16] M. Aydogdu, *A general nonlocal beam theory: Its application to nanobeam bending, buckling and vibration*, Physica E **41** (2009), 1651–1655.

[17] B. Babić, J. Furer, S. Sahoo, S. Farhangfar, and C. Schönenberger, *Intrinsic thermal vibrations of suspended doubly clamped single-wall carbon nanotubes*, Nano Lett. **3** (2003), 1577–1580.

[18] S. M. Bağdatli, *Non-linear vibration of nanobeams with various boundary condition based on nonlocal elasticity theory*, Compos. Part B Eng. **80** (2015), 43–52.

[19] A. Bahrami, *Free vibration, wave power transmission and reflection in multi-cracked nanorods*, Compos. Part B Eng. **127** (2017), 53–62.

[20] E. Barkanov, E. Skukis, and B. Petitjean, *Characterisation of viscoelastic layers in sandwich panels via an inverse technique*, J. Sound Vib. **327** (2009), 402–412.

[21] L. Behera and S. Chakraverty, *Application of differential quadrature method in free vibration analysis of nanobeams based on various nonlocal theories*, Comput. Math. Appl. **69** (2015), 1444–1462.

[22] L. Behera and S. Chakraverty, *Recent researches on nonlocal elasticity theory in the vibration of carbon nanotubes using beam models: A review*, Arch Comput. Methods **24** (2017), 481–494.

[23] M. O. Belarbi, A. A. Daikh, A. Garg, T. Merzouki, H. D. Chalak, and H. Hirane, *Nonlocal finite element model for the bending and buckling analysis of functionally graded nanobeams using a novel shear deformation theory*, Compos. Struct. **264** (2021), 113712.

[24] K. B. Broberg, *Cracks and Fracture*, Elsevier, 1999.

[25] D. Broek, *The Practical Use of Fracture Mechanics*, Springer Science & Business Media, 2012.

[26] F. Cannizzaro, I. Fiore, A. Greco, S. Caddemi, and I. Caliò, *Eigenproperties of multi-cracked circular arches*, J. Sound Vib. **543** (2023), 117365.

[27] M. N. Cerri, M. Dilena, and G. C. Ruta, *Vibration and damage detection in undamaged and cracked circular arches: Experimental and analytical results*, J. Sound Vib. **314** (2008), 83–94.

[28] M. N. Cerri and G. C. Ruta, *Detection of localised damage in plane circular arches by frequency data*, J. Sound Vib. **270** (2004), 39–59.

[29] P. Chidamparam and A. W. Leissa, *Vibrations of planar curved beams, rings, and arches*, Appl. Mech. Reviews **46** (1993), 467–483.

[30] S. S. B. Chinka, S. R. Putti, and B. K. Adavi, *Modal testing and evaluation of cracks on cantilever beam using mode shape curvatures and natural frequencies*, Structures **32** (2021), 1386–1397.

[31] T. G. Chondros, A. D. Dimarogonas, and J. Yao, *A continuous cracked beam vibration theory*, J. Sound Vib. **215** (1998), 17–34.

[32] T. G. Chondros, A. D. Dimarogonas, and J. Yao, *Vibration of a beam with a breathing crack*, J. Sound Vib. **239** (2001), 57–67.

[33] O. Civalek and C. Demir, *Bending analysis of microtubules using nonlocal Euler–Bernoulli beam theory*, Appl. Math. Model. **35** (2011), 2053–2067.

[34] H. Dai, J. H. Hafner, A. G. Rinzler, D. T. Colbert, and R. E. Smalley, *Nanotubes as nanoprobes in scanning probe microscopy*, Nature **384** (1996), 147–150.

[35] C. Demir, O. Civalek, and B. Akgöz, *Free vibration analysis of carbon nanotubes based on shear deformable beam theory by discrete singular convolution technique*, Math. Comput. Appl. **15** (2010), 57–65.

[36] J.P. Den Hartog, *Xl. the lowest natural frequency of circular arcs*, Phil. Mag. **5** (1928), 400–408.

[37] A. D. Dimarogonas, *Vibration of cracked structures: A state of the art review*, Eng. Fract. Mech. **55** (1996), 831–857.

[38] A. D. Dimarogonas, S. A. Paipetis, and T. G. Chondros, *Analytical Methods in Rotor Dynamics*, Springer Science & Business Media, 2013.

[39] W. H. Duan, Q. Wang, K. M. Liew, and X. Q. He, *Molecular mechanics modeling of carbon nanotube fracture*, Carbon **45** (2007), 1769–1776.

[40] F. Ebrahimi and M. R. Barati, *A nonlocal strain gradient refined beam model for buckling analysis of size-dependent shear-deformable curved FG nanobeams*, Comp. Struc. **159** (2017), 174–182.

[41] F. Ebrahimi and M. Daman, *Investigating surface effects on thermomechanical behavior of embedded circular curved nanosize beams*, J. Eng. **2016** (2016).

[42] F. Ebrahimi and M. R. Barati, *Magneto-electro-elastic buckling analysis of nonlocal curved nanobeams*, Eur. Phys. J. Plus. **131** (2016), 1–13.

[43] F. Ebrahimi and M. R. Barati, *On nonlocal characteristics of curved inhomogeneous Euler–Bernoulli nanobeams under different temperature distributions*, Appl. Phys. A **122** (2016), 1–11.

[44] M. C. Ece, M. Aydogdu, and V. Taskin, *Vibration of a variable cross-section beam*, Mech. Res. Commun. **34** (2007), 78–84.

[45] D. S. Eddy and D. R. Sparks, *Application of MEMS technology in automotive sensors and actuators*, Proc. IEEE **86** (1998), 1747–1755.

[46] A. C. Eringen, *Nonlocal Continuum Field Theories, Springer, Berlin*, (2002).

[47] A. C. Eringen and D. G. B. Edelen, *On nonlocal elasticity*, Int. J. Eng. Sci. **10** (1972), 233–248.

[48] U. Eroglu and E. Tufekci, *Exact solution based finite element formulation of cracked beams for crack detection*, Int. J. Solids Struct. **96** (2016), 240–253.

[49] L. B. Freund and G. Herrmann, *Dynamic Fracture of a Beam or Plate in Plane Bending*, (1976).

[50] M. Ganapathi, T. Merzouki, and O. Polit, *Vibration study of curved nanobeams based on nonlocal higher-order shear deformation theory using finite element approach*, Compos. Struct. **184** (2018), 821–838.

[51] M. Ganapathi and O. Polit, *A nonlocal higher-order model including thickness stretching effect for bending and buckling of curved nanobeams*, Appl. Math. Model. **57** (2018), 121–141.

[52] E. E. Gdoutos, *Fracture Mechanics Criteria and Applications*, Springer Science & Business Media, 2012.

[53] E. E. Gdoutos, *Fracture Mechanics: An Introduction*, Springer Nature, 2020.

[54] R. F. Gibson, E. O. Ayorinde, and Y. F. Wen, *Vibrations of carbon nanotubes and their composites: a review*, Compos. Sci. Technol. **67** (2007), 1–28.

[55] D. Gross, *Some Remarks on the History of Fracture Mechanics*, Springer, 2014.

[56] SS Gupta, FG Bosco, and RC Batra, *Wall thickness and elastic moduli of single-walled carbon nanotubes from frequencies of axial, torsional and inextensional modes of vibration*, Comput. Mater. Sci. **47** (2010), no. 4, 1049–1059.

[57] S. H. Hashemi, M. Fakher, R. Nazemnezhad, and M. H. S. Haghighi, *Dynamic behavior of thin and thick cracked nanobeams incorporating surface effects*, Compos. Part B Eng. **61** (2014), 66–72.

[58] S. M. Hasheminejad, B. Gheshlaghi, Y. Mirzaei, and S. Abbasion, *Free transverse vibrations of cracked nanobeams with surface effects*, Thin Solid Films **519** (2011), 2477–2482.

[59] G. D. Hatzigeorgiou and D. E. Beskos, *Inelastic response of 3-D underground structures in rock under seismic loading*, WIT Trans. Built Environment **57** (2001).

[60] J. Heyman, *The stone skeleton*, Int. J. Solids Struct. **2** (1966), 249–279.

[61] M. M. Hossain and J. Lellep, *Mode shape analysis of dynamic behaviour of cracked nanobeam on elastic foundation*, Eng. Res. Express **3** (2021), 045003.

[62] M. Hosseini, A. Hadi, A. Malekshahi, and M. Shishesaz, *A review of size-dependent elasticity for nanostructures*, J. Comput. Appl. Mech. **49** (2018), 197–211.

[63] S. A. H. Hosseini and O. Rahmani, *Free vibration of shallow and deep curved FG nanobeam via nonlocal Timoshenko curved beam model*, Appl. Phys. **122** (2016), 1–11.

[64] M. H. Hsu, *Vibration analysis of edge-cracked beam on elastic foundation with axial loading using the differential quadrature method*, Comput. Methods Appl. Mech. Eng. **194** (2005), 1–17.

[65] R. M. Jones, *Buckling of Bars, Plates, and Shells*, Bull Ridge Corporation, 2006.

[66] C. Journet, M. Picher, and V. Jourdain, *Carbon nanotube synthesis: From large-scale production to atom-by-atom growth*, Nanotechnol. **23** (2012), 142001.

[67] Z. Kala, *Estimating probability of fatigue failure of steel structures*, Acta Comment. Univ. Tartu. Math. **23** (2019), 245–254.

[68] C. Karaagac, H. Ozturk, and M. Sabuncu, *Free vibration and lateral buckling of a cantilever slender beam with an edge crack: Experimental and numerical studies*, J. Sound Vib. **326** (2009), 235–250.

[69] C. Karaagac, H. Ozturk, and M. Sabuncu, *Crack effects on the in-plane static and dynamic stabilities of a curved beam with an edge crack*, J. Sound Vib. **330** (2011), 1718–1736.

[70] B. Karami and M. Janghorban, *A new size-dependent shear deformation theory for free vibration analysis of functionally*

graded/anisotropic nanobeams, Thin-Walled Struct. **143** (2019), 106227.

[71] G. Karami and P. Malekzadeh, *In-plane free vibration analysis of circular arches with varying cross-sections using differential quadrature method*, J. Sound Vib. **274** (2004), 777–799.

[72] L. L. Ke, Y. S. Wang, J. Yang, and S. Kitipornchai, *Free vibration of size-dependent magneto-electro-elastic nanoplates based on the nonlocal theory*, Acta Mech. Sin. **30** (2014), 516–525.

[73] S. J. A. Koh and H. P. Lee, *Molecular dynamics simulation of size and strain rate dependent mechanical response of FCC metallic nanowires*, Nanotech. **17** (2006), 3451.

[74] M. Krawczuk, W. Ostachowicz, and A. Zak, *Dynamics of cracked composite material structures*, Comp. Mech. **20** (1997), 79–83.

[75] S. Kukla, *Free vibrations and stability of stepped columns with cracks*, J. Sound Vib. **319** (2009), 1301–1311.

[76] R. Kumar and S. K. Singh, *Crack detection near the ends of a beam using wavelet transform and high resolution beam deflection measurement*, Eur. J. Mech. A/Solids. **88** (2021), 104259.

[77] P. A. Laura and M. J. Maurizi, *Recent research on vibrations of arch-type structures*, Shock Vib. Digest **19** (1987), 6–9.

[78] B. K. Lee and J. F. Wilson, *Free vibrations of arches with variable curvature*, J. Sound Vib. **136** (1990), 75–89.

[79] J. Lellep and E. Kägo, *Vibrations of elastic stretched strips with cracks*, Int. J. Mech **5** (2011), 27–34.

[80] J. Lellep and A. Lenbaum, *Free vibrations of stepped nano-beams with cracks*, Proc. Estonian Acad. Sci. **71** (2022), 103–116.

[81] J. Lellep and A. Lenbaum, *Free vibrations of stepped nano-beams*, Int. J. Comp. Meth. and Exp. Meas. **6** (2018), 716–725.

[82] J. Lellep and A. Lenbaum, *Natural vibrations of stepped nanobeams with defects*, Acta Comment. Univ. Tartu. Math. **23** (2019), 143–158.

[83] J. Lellep and A. Liyvapuu, *Natural vibrations of stepped arches with cracks*, Agron. Res. **14** (2016), 821–830.

[84] J. Lellep and S. Mubasshar, *Natural vibrations of curved nanobeams and nano-arches*, Acta Comment. Math. Tartu **26** (2022), 63–76.

[85] J. Lellep and E. Sakkov, *Buckling of stepped composite columns*, Mech. Compos. Mater. **42** (2006), 63–72.

[86] C. Li, L. Yao, W. Chen, and S. Li, *Comments on nonlocal effects in nano-cantilever beams*, Int. J. Eng. Sci. **87** (2015), 47–57.

[87] G. Li, Y. Xing, Z. Wang, and Q. Sun, *Effect of boundary conditions and constitutive relations on the free vibration of nonlocal beams*, Res. Phys. **19** (2020), 103414.

[88] S. Li and G. Wang, *Introduction to Micromechanics and Nanomechanics*, World Scientific Publishing Company, 2008.

[89] Z. Li, Y. Xu, and D. Huang, *Analytical solution for vibration of functionally graded beams with variable cross-sections resting on pasternak elastic foundations*, Int. J. Mech. Sci. **191** (2021), 106084.

[90] Y. S. Lim, J. G. Ahn, T. Joo, K. J. Yee, E. H. Haroz, L. G. Booshehri, and J. Kono, *Coherent lattice vibrations in small diameter single-walled carbon nanotubes*, Int. Quantum Electr. Conf., Optica Publishing Group, 2009.

[91] Y. S. Lim, K. J. Yee, J. H. Kim, E. H. Haroz, J. Shaver, J. Kono, S. K. Doorn, R. H. Hauge, and R. E. Smalley, *Coherent lattice vibrations in single-walled carbon nanotubes*, Nano Lett. **6** (2006), 2696–2700.

[92] M. Loghmani and M. R. H. Yazdi, *An analytical method for free vibration of multi cracked and stepped nonlocal nanobeams based on wave approach*, Res. Phys. **11** (2018), 166–181.

[93] J. Logo, *New type of optimality criteria method in case of probabilistic loading conditions*, Mech. Based Des. Struct. Mach. **35** (2007), 147–162.

[94] A. E. H. Love, *A Treatise on the Mathematical Theory of Elasticity*, University Press, 1927.

[95] J. Loya, J. L. Puente, R. Zaera, and J. F. Sáez, *Free transverse vibrations of cracked nanobeams using a nonlocal elasticity model*, J. Appl. Phys. **105** (2009), 044309.

[96] C. Lozano, G. Lumay, I. Zuriguel, R. C. Hidalgo, and A. Garcimartín, *Breaking arches with vibrations: The role of defects*, Phys. Rev. Lett. **109** (2012), 068001.

[97] F. F. Mahmoud, M. A. Eltaher, A. E. Alshorbagy, and E. I. Meletis, *Static analysis of nanobeams including surface effects by nonlocal finite element*, J. Mech. Sci. Technol. **26** (2012), 3555–3563.

[98] A. Majeed, A. Zeeshan, and S. Mubbashir, *Vibration analysis of carbon nanotubes based on cylindrical shell by inducting Winkler and Pasternak foundations*, Mech. Adv. Mater. Struct. **26** (2019), 1140–1145.

[99] A. Maknickas, V. Alekna, O. Ardatov, O. Chabarova, D. Zabulionis, M. Tamulaitienė, and R. Kačianauskas, *FEM-based compression fracture risk assessment in osteoporotic lumbar vertebra l1*, Appl. Sci. **9** (2019), 3013.

[100] A. E. Mamaghani, H. Sarparast, and M. Rezaei, *On the vibrations of axially graded Rayleigh beams under a moving load*, Appl. Math. Model. **84** (2020), 554–570.

[101] M. S. Marefat, E. Ghahremani-Gargary, and S. Ataei, *Load test of a plain concrete arch railway bridge of 20-m span*, Constr. Build. Mater. **18** (2004), 661–667.

[102] K. Mazanoglu and M. Sabuncu, *Flexural vibration of non-uniform beams having double-edge breathing cracks*, J. Sound Vib. **329** (2010), 4181–4191.

[103] K. Mazanoglu, I. Yesilyurt, and M. Sabuncu, *Vibration analysis of multiple-cracked non-uniform beams*, J. Sound Vib. **320** (2009), 977–989.

[104] B. F. Monea, E. I. Ionete, S. I. Spiridon, D. Ion-Ebrasu, and E. Petre, *Carbon nanotubes and carbon nanotube structures used for temperature measurement*, Sensors **19** (2019), 2464.

[105] H. Moosavi, M. Mohammadi, A. Farajpour, and S. H. Shahidi, *Vibration analysis of nanorings using nonlocal continuum mechanics and shear deformable ring theory*, Physica E **44** (2011), 135–140.

[106] T. Murmu and S. C. Pradhan, *Small-scale effect on the free in-plane vibration of nanoplates by nonlocal continuum model*, Physica E **41** (2009), 1628–1633.

[107] C. Y. Nam, P. Jaroenapibal, D. Tham, D. E Luzzi, S. Evoy, and J. E. Fischer, *Diameter-dependent electromechanical properties of GaN nanowires*, Nano Lett. **6** (2006), 153–158.

[108] K. H. Ng and C. A. Fairfield, *Modifying the mechanism method of masonry arch bridge analysis*, Constr. Build. Mater. **18** (2004), 91–97.

[109] N. T. Nguyen, X. Huang, and T. K. Chuan, *MEMS-micropumps: A review*, J. Fluids Eng. **124** (2002), 384–392.

[110] Z. Ni and H. Hua, *Axial-bending coupled vibration analysis of an axially-loaded stepped multi-layered beam with arbitrary boundary conditions*, Int. J. Mech. Sci. **138** (2018), 187–198.

[111] Q. H. Pham, V. K. Tran, T. T. Tran, T. Nguyen-Thoi, P. C. Nguyen, and V. D. Pham, *A nonlocal quasi-3D theory for thermal free vibration analysis of functionally graded material nanoplates rest-*

ing on elastic foundation, Case Stud. Therm. Eng. **26** (2021), 101170.

[112] O. Polit, T. Merzouki, and M. Ganapathi, *Elastic stability of curved nanobeam based on higher-order shear deformation theory and nonlocal analysis by finite element approach*, Finite Elem. Anal. Des. **146** (2018), 1–15.

[113] W. Qiao, T. Guo, H. Kang, and Y. Zhao, *An asymptotic study of nonlinear coupled vibration of arch-foundation structural system*, Eur. J. Mech. A-Solids. **96** (2022), 104711.

[114] S. Rajasekaran and H. B. Khaniki, *Size-dependent forced vibration of non-uniform bi-directional functionally graded beams embedded in variable elastic environment carrying a moving harmonic mass*, Appl. Math. Modell. **72** (2019), 129–154.

[115] J. N. Reddy, *Nonlocal theories for bending, buckling and vibration of beams*, Int. J. Eng. Sci. **45** (2007), 288–307.

[116] J. N. Reddy and S. D. Pang, *Nonlocal continuum theories of beams for the analysis of carbon nanotubes*, J. Appl. Phys. **103** (2008), 023511.

[117] M. Rezaiee-Pajand and N. Rajabzadeh-Safaei, *Nonlocal static analysis of a functionally graded material curved nanobeam*, Mech. Adv. Mater. Struct. **25** (2018), 539–547.

[118] J. R. Rice, *A path independent integral and the approximate analysis of strain concentration by notches and cracks*, J. Appl. Mech. **35** (1968), 379–386.

[119] P. F. Rizos, N. Aspragathos, and A. D. Dimarogonas, *Identification of crack location and magnitude in a cantilever beam from the vibration modes*, J. Sound Vib. **138** (1990), 381–388.

[120] H. Roostai and M. Haghpanahi, *Vibration of nanobeams of different boundary conditions with multiple cracks based on nonlocal elasticity theory*, Appl. Math. Model. **38** (2014), 1159–1169.

[121] C. M. C. Roque, A. J. M. Ferreira, and J. N. Reddy, *Analysis of Timoshenko nanobeams with a nonlocal formulation and meshless method*, Int. J. Eng. Sci. **49** (2011), 976–984.

[122] M. A. D. Rosa and M. Lippiello, *Closed-form solutions for vibrations analysis of cracked Timoshenko beams on elastic medium: An analytical approach*, Eng. Struct. **236** (2021), 111946.

[123] S. Sahmani and R. Ansari, *Nonlocal beam models for buckling of nanobeams using state-space method regarding different boundary conditions*, J. Mech. Sci. Technol. **25** (2011), 2365–2375.

[124] S. Šalinić, A. Obradović, and A. Tomović, *Free vibration analysis of axially functionally graded tapered, stepped, and continuously segmented rods and beams*, Compos. Part B Eng. **150** (2018), 135–143.

[125] S. Sen and L. Khazanovich, *A self-contained element for modeling crack propagation in beams*, Eng. Fract. Mech. **242** (2021), 107460.

[126] G. L. She, H. B. Liu, and B. Karami, *On resonance behavior of porous FG curved nanobeams*, Steel Compos. Struct **36** (2020), 179–186.

[127] Y. Shi, C. Q. Chen, Y. S. Zhang, J. Zhu, and Y. J. Yan, *Determination of the natural frequency of a cantilevered ZnO nanowire resonantly excited by a sinusoidal electric field*, Nanotech. **18** (2007), 075709.

[128] M. Şimşek, *Nonlinear free vibration of a functionally graded nanobeam using nonlocal strain gradient theory and a novel hamiltonian approach*, Int. J. Eng. Sci. **105** (2016), 12–27.

[129] W. Soedel, *Vibrations of Shells and Plates*, Marcel Dekker, NY, 2004.

[130] M. Song, Y. Gong, J. Yang, W. Zhu, and S. Kitipornchai, *Nonlinear free vibration of cracked functionally graded graphene*

platelet-reinforced nanocomposite beams in thermal environments, J. Sound Vib. **468** (2020), 115115.

[131] Z. Su, G. Jin, and T. Ye, *Vibration analysis of multiple-stepped functionally graded beams with general boundary conditions*, Compos. Struct. **186** (2018), 315–323.

[132] A. S. Surla, S. Y. Kang, and J. S. Park, *Inelastic buckling assessment of monosymmetric I-beams having stepped and non-compact flange sections*, J. Constr. Steel Res. **114** (2015), 325–337.

[133] H. Tada, P. C. Paris, and G. R. Irwin, *The Stress Analysis of Cracks*, Handbook, Del Research Corporation **34** (1973).

[134] H. T. Thai, *A nonlocal beam theory for bending, buckling, and vibration of nanobeams*, Int. J. Eng. Sci. **52** (2012), 56–64.

[135] H. T. Thai, T. P. Vo, T. K. Nguyen, and S. E. Kim, *A review of continuum mechanics models for size-dependent analysis of beams and plates*, Compos. Struct. **177** (2017), 196–219.

[136] S. Timoshenko, *History of Strength of Materials: With a Brief Account of the History of Theory of Elasticity and Theory of Structures*, Courier Corporation, 1983.

[137] K. Torabi and J. N. Dastgerdi, *An analytical method for free vibration analysis of Timoshenko beam theory applied to cracked nanobeams using a nonlocal elasticity model*, Thin Solid Films **520** (2012), 6595–6602.

[138] J. Tretjakovas, R. Kačianauskas, and C. Šimkevičius, *FE simulation of rupture of diaphragm with initiated defect*, Mechanics **62** (2006), 5–10.

[139] E. Viola, E. Artioli, and M. Dilena, *Analytical and differential quadrature results for vibration analysis of damaged circular arches*, J. Sound Vib. **288** (2005), 887–906.

[140] E. Viola and F. Tornabene, *Free vibrations of three parameter functionally graded parabolic panels of revolution*, Mech. Res. Commun. **36** (2009), 587–594.

[141] C. M. Wang and W. H. Duan, *Free vibration of nanorings/arches based on nonlocal elasticity*, J. Appl. Phys. **104** (2008), 014303.

[142] C. M. Wang, V. B. C. Tan, and Y. Y. Zhang, *Timoshenko beam model for vibration analysis of multi-walled carbon nanotubes*, J. Sound Vib. **294** (2006), 1060–1072.

[143] C. M. Wang, Y. Xiang, J. Yang, and S. Kitipornchai, *Buckling of nano-rings/arches based on nonlocal elasticity*, Int. J. Appl. Mech. **4** (2012), 1250025.

[144] C. M. Wang, H. Zhang, N. Challamel, and W. H. Duan, *On boundary conditions for buckling and vibration of nonlocal beams*, Eur. J. Mech. A-Solids **61** (2017), 73–81.

[145] C. M. Wang, Y. Y. Zhang, and X. Q. He, *Vibration of nonlocal Timoshenko beams*, Nanotech. **18** (2007), 105401.

[146] C. M. Wang, Y. Y. Zhang, S. S. Ramesh, and S. Kitipornchai, *Buckling analysis of micro-and nano-rods/tubes based on nonlocal Timoshenko beam theory*, J. Phys. D: Appl. Phys. **39** (2006), 3904.

[147] Q. Wang and B. Arash, *A review on applications of carbon nanotubes and graphenes as nano-resonator sensors*, Computa. Mate. Sci. **82** (2014), 350–360.

[148] Q. Wang, W. H. Duan, N. L. Richards, and K. M. Liew, *Modeling of fracture of carbon nanotubes with vacancy defect*, Phys. Rev. B **75** (2007), 201405.

[149] C. P. Wu and J. J. Yu, *A review of mechanical analyses of rectangular nanobeams and single-, double-, and multi-walled carbon nanotubes using Eringen's nonlocal elasticity theory*, Arch. Appl. Mech. **89** (2019), 1761–1792.

[150] J. S. Wu and L. K. Chiang, *A new approach for free vibration analysis of arches with effects of shear deformation and rotary inertia considered*, J. Sound Vib. **277** (2004), 49–71.

[151] Q. Wu, S. Guo, X. Li, and G. Gao, *Crack diagnosis method for a cantilevered beam structure based on modal parameters*, Meas. Sci. Technol. **31** (2019), 035001.

[152] Y. Yan, B. Liu, Y. Xing, E. Carrera, and A. Pagani, *Free vibration analysis of variable stiffness composite laminated beams and plates by novel hierarchical differential quadrature finite elements*, Compos. Struct. **274** (2021), 114364.

[153] A. Yavari and S. Sarkani, *On applications of generalized functions to the analysis of Euler–Bernoulli beam–columns with jump discontinuities*, Int. J. Mech. Sci. **43** (2001), 1543–1562.

[154] D. J. Zeng and Q. S. Zheng, *Resonant frequency-based method for measuring the Young's moduli of nanowires*, Phys. Rev. B **76** (2007), 075417.

[155] A. M. Zenkour and A. F. Radwan, *A compressive study for porous FG curved nanobeam under various boundary conditions via a nonlocal strain gradient theory*, Eur. Phys. J. Plus **136** (2021), 248.

[156] H. Zhang, C. M. Wang, and N. Challamel, *Small length scale coefficient for Eringen's and lattice-based continualized nonlocal circular arches in buckling and vibration*, Comp. Struct. **165** (2017), 148–159.

[157] Y. F. Zhang, Y. Niu, and W. Zhang, *Nonlinear vibrations and internal resonance of pretwisted rotating cantilever rectangular plate with varying cross-section and aerodynamic force*, Eng. Struct. **225** (2020), 111259.

[158] L. Zhou and Y. Huang, *Crack effect on the elastic buckling behavior of axially and eccentrically loaded columns*, Struct. Eng. Mech. **22** (2006), 169–184.

Summary

The natural vibrations of curved nanobeams or nanoarches are studied in the present work. To achieve authentic results, the study employs the nonlocal theory of elasticity, which accounts for small-length scale effects that are not considered by the classical theory. The impact of crack-like defects on the natural frequency is thoroughly examined, and the obtained results are compared with available data.

Nanoarches with constant thickness, where a stable crack is located within the element are studied first of all. Additionally, nanoarches with piecewise constant thickness are analysed, where stable cracks are positioned at the re-entrant corners of steps. A novel method based on linear elastic fracture mechanics is developed to determine the natural frequencies of nanoarches. Different nanoarches such as simply supported, clamped at both edges and cantilevers are considered. The method developed in this study is also applied to investigate the vibrational behaviour of the CNTs of the shapes armchair, zigzag and chiral.

To solve the governing equations, a numerical approach utilising the separation of variables is employed. The obtained results are validated by comparing them with existing literature. Furthermore, the study emphasizes the significant role of cracks in altering the frequency behaviour of curved beams.

Moreover, the research extensively discusses the influence of various parameters, including thickness, radius and central angle on the eigenfrequency of the nanoarches.

The dissertation is organised as follows:

Chapter 1 provides a historical review of the papers on the natural vibrations of curved nanobeams, focusing on the application of Eringen's nonlocal theory of elasticity. In Chapter 2, the physical model of the nanoarch is presented. The model includes both defects and steps. The governing equations required for analysing the natural frequency of the nanoarch are also presented in Chapter 2. The natural frequency of the nanoarches of constant thickness is defined in Chapter 2. The natural frequency of the simply supported nanoarches of piecewise constant thickness with a defect is presented in Chapter 4. Chapter 5 focuses on

the natural frequency of the nanoarch with both a flaw and a step, considering clamped nanoarches. In Chapter 6, the natural frequency of the cantilever nanoarches is determined. In Chapter 7, the method developed in this study is applied to analyse the natural vibrations of CNTs. Finally, the concluding remarks of the dissertation summarising the key findings and contributions of the research work are provided.

Summary in Estonian

Kõverate nanotalade vabavõnkumised

Antud uurimistöö keskendub kõverate nanokaarte omavõnkumistele. Töös kasutatakse elastsuse teooriat, mis võtab arvesse mõjusid, mida klassikaline teooria ei arvesta. Siin uuritakse prao-tüüpi defektide mõju omavõnkesagedusele.

Põhivõrrandite lahendamiseks kasutatakse numbrilist meetodit, mis põhineb muutujate eraldamisel. Saadud tulemusi võrreldakse kirjanduses leiduvate tulemustega. Lisaks uuritakse erinevate füüsikaliste ja geomeetriliste parameetrite, sealhulgas paksuse, raadiuse ja kaare kesknurga mõju vaba võnkumise sagedusele.

Doktoritöö põhineb autori koostatud viiel publikatsioonil, millest üks on avaldatud ning teised on trükki suunatud. Doktoritöö struktuur hõlmab kirjanduse ülevaadet, sisu lühikokkuvõtet, kirjanduse loetelu ja autori elulookirjeldust.

Doktoritöö on korraldatud järgmiselt:

Esimeses peatükis antakse ajalooline ülevaade kõverate nano-talade omavõnkumiste uurimisest keskendudes Eringeni mitteokaalse elastilisuse teooria rakendamisele. Esitatakse nanokaare füüsikaline mudel, arvestades nii defekte kui ka astmeid, ning esitatakse sageduste leidmiseks vajalikud võrrandid. Teises peatükis kirjeldatakse uuritavat nanokaare mudelit, kus paksus on tükiti konstantne ning millel on praod paksuse hüppekohtades. Kolmandas peatükis leitakse konstantse paksusega kõvera nanotala omavõnkesagedused vabalt toetatud ja jäigalt kinnitatud otste korral. Neljandas ja vüendas peatükis leitakse omavõnkesagedused astmeliste nanokaarte jaoks, millel on defektid. Kuues peatükk on pühendatud niisuguste nanokaarte uurimisele, mille üks ots on jäigalt kinnitatud ja teine täiesti vaba. Viimases osas esitatakse saadud tulemuste põhjal tehtud järeldused.

Acknowledgements

First and foremost, I would like to express my sincere gratitude to my supervisor, Prof. Jaan Lellep. His support and invaluable guidance have been instrumental throughout this study. Especially the time he devoted to discussions and corrections of this manuscript helped me to prepare it. Without his expertise and kindness, I would not have been able to complete this dissertation successfully.

I would also like to extend my appreciation to all faculty members, especially the head of the institute, Assoc. Prof. Meelis Käärik, Prof. Rainis Haller and Johann Langemets for their support and guidance. I am also thankful to all the secretaries and colleagues who have played a significant role in managing this study. I would like to mention Evely Kirsiaed and Julia Polikarpus, who have provided valuable guidance and assistance during the course of my research.

I would also like to acknowledge the contributions of my colleagues and friends, especially Junming Ke and Anastassia Kolde, whose company and support have made my stay in Estonia remarkable and enjoyable.

Lastly, I am deeply grateful to my family members, especially my parents, for their unwavering support throughout this course. Their encouragement and understanding have been incredibly helpful in navigating the challenges of this journey.

Curriculum Vitae

Name: Shahid Mubasshar
Date and place of birth: January 1, 1993, Jallah Jeem, Punjab, Pakistan
Nationality: Pakistan
Email: smsaroya47@gmail.com, shahid@ut.ee
LinkedIn profile: Shahid Mubasshar

Employment

Junior Research Fellow, 11/2021 to Current time
University of Tartu – Tartu, Estonia
Teaching Assistant, 09/2020 to 02/2021
University of Tartu – Tartu, Estonia
Lecturer, Mathematics, 06/2017 to 07/2019
Modern Language Schools and Colleges – Islamabad, Pakistan

Education & Certificates

Ph.D.: Mathematics, In progress
University of Tartu – Estonia
Master of Science: Applied Mathematics, 08/2017
International Islamic University – Islamabad, Pakistan
Bachelor of Science: Mathematics, Physics, 07/2014
International Islamic University – Islamabad, Pakistan
Student Ambassador: Autumn Semester, 2023
Baltic University Program
Short training: How to use Atomic Force Microscope, March 2023
Jagiellonian University – Krakow, Poland

Summer School under ClimateKic, July-December 2022
Lisbon, Portugal

Publications

- J. Lellep and S. Mubasshar, Nonlocal theory of elasticity in the natural vibrations of curved CNTs with defects, Proc. Conf. Indust. Appl. Math. (submitted)
- J. Lellep and S. Mubasshar, Natural vibrations of circular nanoarches of piecewise constant thickness, Acta Comment. Math. Tartu. (submitted)
- J. Lellep and S. Mubasshar, Natural vibrations of nonlocal curved clamped nanobeams. J. Vib. Control. (submitted)
- J. Lellep and S. Mubasshar, Natural vibrations of curved nanobeams and nanoarches, Acta Comment. Math. Tartu 26 (2022),63-76.
- A. Majeed, A. Zeeshan, and S Mubbashir. Vibration analysis of carbon nanotubes based on cylindrical shell by inducting Winkler and Pasternak foundations. Mech. Adv. Mater. Struct. 26(2019), 1140-45.

Conferences Participated

- Fifth Int. Conf. Optimization and Analysis of Structures (OAS 2023)– Tartu, Estonia
- 22^{nd} ECMI Conf. on Industrial and Applied Mathematics 26-30 June 2023 – Wroclaw, Poland
- 2022 Int. Conf. on Applied Mathematics, Informatics, and Computing Sciences (AMICS 2022) – Shanghai, China
- First Int. Conf. of Mathematics and Statistics, International Islamic University, 2018– Islamabad, Pakistan

Elulookirjeldus

Nimi: Shahid Mubasshar
Sünniaeg ja -koht: 1. jaanuar 1993, Jallah Jeem, Punjab, Pakistan
Kodakondsus: Pakistan
E-post: smsaroya47@gmail.com, shahid@ut.ee
LinkedIni profiil: Shahid Mubasshar

Töökogemus

Nooremteadur, 11/2021 kuni praeguseni
Tartu Ülikool – Tartu, Eesti
Õpetajaabi, 09/2020 kuni 02/2021
Tartu Ülikool – Tartu, Eesti
Lektor, matemaatika, 06/2017 kuni 07/2019
Modern Language Schools and Colleges – Islamabad, Pakistan

Haridus & Tunnistused

Ph.D.: Matemaatika, hetkel pooleli
Tartu Ülikool – Eesti
Magistrikraad: Rakendusmatemaatika, 08/2017
International Islamic University – Islamabad, Pakistan
Bakalaureusekraad: Matemaatika, Füüsika, 07/2014
International Islamic University – Islamabad, Pakistan
Üliõpilas-ambassador: Sügissemester, 2023
Baltic University Program
Lühikoolitus: Kuidas kasutada aatomjõumikroskoopi, märts 2023
Jagiellonian University – Krakow, Poola
Suvekool ClimateKic raames, juuli-detsember 2022
Lisbon, Portugal

Artiklid

- J. Lellep and S. Mubasshar, Nonlocal theory of elasticity in the natural vibrations of curved CNTs with defects, Proc. Conf. Indust. Appl. Math. (esitatud)
- J. Lellep and S. Mubasshar, Natural vibrations of circular nanoarches of piecewise constant thickness, Acta Comment. Math. Tartu. (esitatud)
- J. Lellep and S. Mubasshar, Natural vibrations of nonlocal curved clamped nanobeams. J. Vib. Control. (esitatud)
- J. Lellep and S. Mubasshar, Natural vibrations of curved nanobeams and nanoarches, Acta Comment. Math. Tartu 26 (2022),63-–76.
- A. Majeed, A. Zeeshan, and S Mubbashir. Vibration analysis of carbon nanotubes based on cylindrical shell by inducting Winkler and Pasternak foundations. Mech. Adv. Mater. Struct. 26(2019), 1140-45.

Konverentsidel osalemised

- OAS 2023, Tartu, Estonia
- 22. ECMI konverents tööstus- ja rakendusmatemaatikas, 26.-30. juuni 2023 – Wroclaw, Poola
- 2022. aasta rahvusvaheline rakendusmatemaatika, infotehnoloogia ja arvutiteaduste konverents (AMICS 2022) – Shanghai, Hiina
- Esimene rahvusvaheline matemaatika ja statistika konverents, International Islamic University Islamabad, Pakistan, 2018

DISSERTATIONES MATHEMATICAE UNIVERSITATIS TARTUENSIS

1. **Mati Heinloo.** The design of nonhomogeneous spherical vessels, cylindrical tubes and circular discs. Tartu, 1991, 23 p.
2. **Boris Komrakov.** Primitive actions and the Sophus Lie problem. Tartu, 1991, 14 p.
3. **Jaak Heinloo.** Phenomenological (continuum) theory of turbulence. Tartu, 1992, 47 p.
4. **Ants Tauts.** Infinite formulae in intuitionistic logic of higher order. Tartu, 1992, 15 p.
5. **Tarmo Soomere.** Kinetic theory of Rossby waves. Tartu, 1992, 32 p.
6. **Jüri Majak.** Optimization of plastic axisymmetric plates and shells in the case of Von Mises yield condition. Tartu, 1992, 32 p.
7. **Ants Aasma.** Matrix transformations of summability and absolute summability fields of matrix methods. Tartu, 1993, 32 p.
8. **Helle Hein.** Optimization of plastic axisymmetric plates and shells with piece-wise constant thickness. Tartu, 1993, 28 p.
9. **Toomas Kiho.** Study of optimality of iterated Lavrentiev method and its generalizations. Tartu, 1994, 23 p.
10. **Arne Kokk.** Joint spectral theory and extension of non-trivial multiplicative linear functionals. Tartu, 1995, 165 p.
11. **Toomas Lepikult.** Automated calculation of dynamically loaded rigid-plastic structures. Tartu, 1995, 93 p, (in Russian).
12. **Sander Hannus.** Parametrical optimization of the plastic cylindrical shells by taking into account geometrical and physical nonlinearities. Tartu, 1995, 74 p, (in Russian).
13. **Sergei Tupailo.** Hilbert's epsilon-symbol in predicative subsystems of analysis. Tartu, 1996, 134 p.
14. **Enno Saks.** Analysis and optimization of elastic-plastic shafts in torsion. Tartu, 1996, 96 p.
15. **Valdis Laan.** Pullbacks and flatness properties of acts. Tartu, 1999, 90 p.
16. **Märt Põldvere.** Subspaces of Banach spaces having Phelps' uniqueness property. Tartu, 1999, 74 p.
17. **Jelena Ausekle.** Compactness of operators in Lorentz and Orlicz sequence spaces. Tartu, 1999, 72 p.
18. **Krista Fischer.** Structural mean models for analyzing the effect of compliance in clinical trials. Tartu, 1999, 124 p.
19. **Helger Lipmaa.** Secure and efficient time-stamping systems. Tartu, 1999, 56 p.
20. **Jüri Lember.** Consistency of empirical k-centres. Tartu, 1999, 148 p.
21. **Ella Puman.** Optimization of plastic conical shells. Tartu, 2000, 102 p.
22. **Kaili Müürisep.** Eesti keele arvutigrammatika: süntaks. Tartu, 2000, 107 lk.

23. **Varmo Vene.** Categorical programming with inductive and coinductive types. Tartu, 2000, 116 p.
24. **Olga Sokratova.** Ω-rings, their flat and projective acts with some applications. Tartu, 2000, 120 p.
25. **Maria Zeltser.** Investigation of double sequence spaces by soft and hard analitical methods. Tartu, 2001, 154 p.
26. **Ernst Tungel.** Optimization of plastic spherical shells. Tartu, 2001, 90 p.
27. **Tiina Puolakainen.** Eesti keele arvutigrammatika: morfoloogiline ühestamine. Tartu, 2001, 138 p.
28. **Rainis Haller.** *M(r,s)*-inequalities. Tartu, 2002, 78 p.
29. **Jan Villemson.** Size-efficient interval time stamps. Tartu, 2002, 82 p.
30. Töö kaitsmata.
31. **Mart Abel.** Structure of Gelfand-Mazur algebras. Tartu, 2003. 94 p.
32. **Vladimir Kuchmei.** Affine completeness of some ockham algebras. Tartu, 2003. 100 p.
33. **Olga Dunajeva.** Asymptotic matrix methods in statistical inference problems. Tartu 2003. 78 p.
34. **Mare Tarang.** Stability of the spline collocation method for volterra integro-differential equations. Tartu 2004. 90 p.
35. **Tatjana Nahtman.** Permutation invariance and reparameterizations in linear models. Tartu 2004. 91 p.
36. **Märt Möls.** Linear mixed models with equivalent predictors. Tartu 2004. 70 p.
37. **Kristiina Hakk.** Approximation methods for weakly singular integral equations with discontinuous coefficients. Tartu 2004, 137 p.
38. **Meelis Käärik.** Fitting sets to probability distributions. Tartu 2005, 90 p.
39. **Inga Parts.** Piecewise polynomial collocation methods for solving weakly singular integro-differential equations. Tartu 2005, 140 p.
40. **Natalia Saealle.** Convergence and summability with speed of functional series. Tartu 2005, 91 p.
41. **Tanel Kaart.** The reliability of linear mixed models in genetic studies. Tartu 2006, 124 p.
42. **Kadre Torn.** Shear and bending response of inelastic structures to dynamic load. Tartu 2006, 142 p.
43. **Kristel Mikkor.** Uniform factorisation for compact subsets of Banach spaces of operators. Tartu 2006, 72 p.
44. **Darja Saveljeva.** Quadratic and cubic spline collocation for Volterra integral equations. Tartu 2006, 117 p.
45. **Kristo Heero.** Path planning and learning strategies for mobile robots in dynamic partially unknown environments. Tartu 2006, 123 p.
46. **Annely Mürk.** Optimization of inelastic plates with cracks. Tartu 2006. 137 p.
47. **Annemai Raidjõe.** Sequence spaces defined by modulus functions and superposition operators. Tartu 2006, 97 p.
48. **Olga Panova.** Real Gelfand-Mazur algebras. Tartu 2006, 82 p.

49. **Härmel Nestra.** Iteratively defined transfinite trace semantics and program slicing with respect to them. Tartu 2006, 116 p.
50. **Margus Pihlak.** Approximation of multivariate distribution functions. Tartu 2007, 82 p.
51. **Ene Käärik.** Handling dropouts in repeated measurements using copulas. Tartu 2007, 99 p.
52. **Artur Sepp.** Affine models in mathematical finance: an analytical approach. Tartu 2007, 147 p.
53. **Marina Issakova.** Solving of linear equations, linear inequalities and systems of linear equations in interactive learning environment. Tartu 2007, 170 p.
54. **Kaja Sõstra.** Restriction estimator for domains. Tartu 2007, 104 p.
55. **Kaarel Kaljurand.** Attempto controlled English as a Semantic Web language. Tartu 2007, 162 p.
56. **Mart Anton.** Mechanical modeling of IPMC actuators at large deformations. Tartu 2008, 123 p.
57. **Evely Leetma.** Solution of smoothing problems with obstacles. Tartu 2009, 81 p.
58. **Ants Kaasik.** Estimating ruin probabilities in the Cramér-Lundberg model with heavy-tailed claims. Tartu 2009, 139 p.
59. **Reimo Palm.** Numerical Comparison of Regularization Algorithms for Solving Ill-Posed Problems. Tartu 2010, 105 p.
60. **Indrek Zolk.** The commuting bounded approximation property of Banach spaces. Tartu 2010, 107 p.
61. **Jüri Reimand.** Functional analysis of gene lists, networks and regulatory systems. Tartu 2010, 153 p.
62. **Ahti Peder.** Superpositional Graphs and Finding the Description of Structure by Counting Method. Tartu 2010, 87 p.
63. **Marek Kolk.** Piecewise Polynomial Collocation for Volterra Integral Equations with Singularities. Tartu 2010, 134 p.
64. **Vesal Vojdani.** Static Data Race Analysis of Heap-Manipulating C Programs. Tartu 2010, 137 p.
65. **Larissa Roots.** Free vibrations of stepped cylindrical shells containing cracks. Tartu 2010, 94 p.
66. **Mark Fišel.** Optimizing Statistical Machine Translation via Input Modification. Tartu 2011, 104 p.
67. **Margus Niitsoo**. Black-box Oracle Separation Techniques with Applications in Time-stamping. Tartu 2011, 174 p.
68. **Olga Liivapuu.** Graded q-differential algebras and algebraic models in noncommutative geometry. Tartu 2011, 112 p.
69. **Aleksei Lissitsin.** Convex approximation properties of Banach spaces. Tartu 2011, 107 p.
70. **Lauri Tart.** Morita equivalence of partially ordered semigroups. Tartu 2011, 101 p.
71. **Siim Karus.** Maintainability of XML Transformations. Tartu 2011, 142 p.

72. **Margus Treumuth.** A Framework for Asynchronous Dialogue Systems: Concepts, Issues and Design Aspects. Tartu 2011, 95 p.
73. **Dmitri Lepp.** Solving simplification problems in the domain of exponents, monomials and polynomials in interactive learning environment T-algebra. Tartu 2011, 202 p.
74. **Meelis Kull.** Statistical enrichment analysis in algorithms for studying gene regulation. Tartu 2011, 151 p.
75. **Nadežda Bazunova.** Differential calculus $d^3 = 0$ on binary and ternary associative algebras. Tartu 2011, 99 p.
76. **Natalja Lepik.** Estimation of domains under restrictions built upon generalized regression and synthetic estimators. Tartu 2011, 133 p.
77. **Bingsheng Zhang.** Efficient cryptographic protocols for secure and private remote databases. Tartu 2011, 206 p.
78. **Reina Uba.** Merging business process models. Tartu 2011, 166 p.
79. **Uuno Puus.** Structural performance as a success factor in software development projects – Estonian experience. Tartu 2012, 106 p.
80. **Marje Johanson.** $M(r, s)$-ideals of compact operators. Tartu 2012, 103 p.
81. **Georg Singer.** Web search engines and complex information needs. Tartu 2012, 218 p.
82. **Vitali Retšnoi.** Vector fields and Lie group representations. Tartu 2012, 108 p.
83. **Dan Bogdanov.** Sharemind: programmable secure computations with practical applications. Tartu 2013, 191 p.
84. **Jevgeni Kabanov.** Towards a more productive Java EE ecosystem. Tartu 2013, 151 p.
85. **Erge Ideon**. Rational spline collocation for boundary value problems. Tartu, 2013, 111 p.
86. **Esta Kägo.** Natural vibrations of elastic stepped plates with cracks. Tartu, 2013, 114 p.
87. **Margus Freudenthal.** Simpl: A toolkit for Domain-Specific Language development in enterprise information systems. Tartu, 2013, 151 p.
88. **Boriss Vlassov.** Optimization of stepped plates in the case of smooth yield surfaces. Tartu, 2013, 104 p.
89. **Elina Safiulina.** Parallel and semiparallel space-like submanifolds of low dimension in pseudo-Euclidean space. Tartu, 2013, 85 p.
90. **Raivo Kolde.** Methods for re-using public gene expression data. Tartu, 2014, 121 p.
91. **Vladimir Šor.** Statistical Approach for Memory Leak Detection in Java Applications. Tartu, 2014, 155 p.
92. **Naved Ahmed.** Deriving Security Requirements from Business Process Models. Tartu, 2014, 171 p.
93. **Kerli Orav-Puurand.** Central Part Interpolation Schemes for Weakly Singular Integral Equations. Tartu, 2014, 109 p.
94. **Liina Kamm.** Privacy-preserving statistical analysis using secure multi-party computation. Tartu, 2015, 201 p.

95. **Kaido Lätt.** Singular fractional differential equations and cordial Volterra integral operators. Tartu, 2015, 93 p.
96. **Oleg Košik.** Categorical equivalence in algebra. Tartu, 2015, 84 p.
97. **Kati Ain.** Compactness and null sequences defined by ℓ_p spaces. Tartu, 2015, 90 p.
98. **Helle Hallik.** Rational spline histopolation. Tartu, 2015, 100 p.
99. **Johann Langemets.** Geometrical structure in diameter 2 Banach spaces. Tartu, 2015, 132 p.
100. **Abel Armas Cervantes.** Diagnosing Behavioral Differences between Business Process Models. Tartu, 2015, 193 p.
101. **Fredrik Milani.** On Sub-Processes, Process Variation and their Interplay: An Integrated Divide-and-Conquer Method for Modeling Business Processes with Variation. Tartu, 2015, 164 p.
102. **Huber Raul Flores Macario.** Service-Oriented and Evidence-aware Mobile Cloud Computing. Tartu, 2015, 163 p.
103. **Tauno Metsalu.** Statistical analysis of multivariate data in bioinformatics. Tartu, 2016, 197 p.
104. **Riivo Talviste.** Applying Secure Multi-party Computation in Practice. Tartu, 2016, 144 p.
105. **Md Raknuzzaman.** Noncommutative Galois Extension Approach to Ternary Grassmann Algebra and Graded q-Differential Algebra. Tartu, 2016, 110 p.
106. **Alexander Liyvapuu.** Natural vibrations of elastic stepped arches with cracks. Tartu, 2016, 110 p.
107. **Julia Polikarpus.** Elastic plastic analysis and optimization of axisymmetric plates. Tartu, 2016, 114 p.
108. **Siim Orasmaa.** Explorations of the Problem of Broad-coverage and General Domain Event Analysis: The Estonian Experience. Tartu, 2016, 186 p.
109. **Prastudy Mungkas Fauzi.** Efficient Non-interactive Zero-knowledge Protocols in the CRS Model. Tartu, 2017, 193 p.
110. **Pelle Jakovits.** Adapting Scientific Computing Algorithms to Distributed Computing Frameworks. Tartu, 2017, 168 p.
111. **Anna Leontjeva.** Using Generative Models to Combine Static and Sequential Features for Classification. Tartu, 2017, 167 p.
112. **Mozhgan Pourmoradnasseri.** Some Problems Related to Extensions of Polytopes. Tartu, 2017, 168 p.
113. **Jaak Randmets.** Programming Languages for Secure Multi-party Computation Application Development. Tartu, 2017, 172 p.
114. **Alisa Pankova.** Efficient Multiparty Computation Secure against Covert and Active Adversaries. Tartu, 2017, 316 p.
115. **Tiina Kraav.** Stability of elastic stepped beams with cracks. Tartu, 2017, 126 p.
116. **Toomas Saarsen.** On the Structure and Use of Process Models and Their Interplay. Tartu, 2017, 123 p.

117. **Silja Veidenberg.** Lifting bounded approximation properties from Banach spaces to their dual spaces. Tartu, 2017, 112 p.
118. **Liivika Tee.** Stochastic Chain-Ladder Methods in Non-Life Insurance. Tartu, 2017, 110 p.
119. **Ülo Reimaa.** Non-unital Morita equivalence in a bicategorical setting. Tartu, 2017, 86 p.
120. **Rauni Lillemets.** Generating Systems of Sets and Sequences. Tartu, 2017, 181 p.
121. **Kristjan Korjus.** Analyzing EEG Data and Improving Data Partitioning for Machine Learning Algorithms. Tartu, 2017, 106 p.
122. **Eno Tõnisson.** Differences between Expected Answers and the Answers Offered by Computer Algebra Systems to School Mathematics Equations. Tartu, 2017, 195 p.
123. **Kaur Lumiste.** Improving accuracy of survey estimators by using auxiliary information in data collection and estimation stages. Tartu, 2018, 112 p.
124. **Paul Tammo.** Closed maximal regular one-sided ideals in topological algebras. Tartu, 2018, 112 p.
125. **Mart Kals.** Computational and statistical methods for DNA sequencing data analysis and applications in the Estonian Biobank cohort. Tartu, 2018, 174 p.
126. **Annika Krutto.** Empirical Cumulant Function Based Parameter Estimation in Stable Distributions. Tartu, 2019, 140 p.
127. **Kristi Läll.** Risk scores and their predictive ability for common complex diseases. Tartu, 2019, 118 p.
128. **Gul Wali Shah.** Spline approximations. Tartu, 2019, 85 p.
129. **Mikk Vikerpuur.** Numerical solution of fractional differential equations. Tartu, 2019, 125 p.
130. **Priit Lätt.** Induced 3-Lie superalgebras and their applications in superspace. Tartu, 2020, 114 p.
131. **Sumaira Rehman.** Fast and quasi-fast solvers for weakly singular Fredholm integral equation of the second kind. Tartu, 2020, 105 p.
132. **Rihhard Nadel.** Big slices of the unit ball in Banach spaces. Tartu, 2020, 109 p.
133. **Katriin Pirk.** Diametral diameter two properties, Daugavet-, and Δ-points in Banach spaces. Tartu, 2020, 106 p.
134. **Zahra Alijani**. Fuzzy integral equations of the second kind. Tartu, 2020, 103 1p.
135. **Hina Arif.** Stability analysis of stepped nanobeams with defects. Tartu, 2021, 165 p.
136. **Joonas Sova.** Pairwise Markov Models. Tartu, 2021, 166 p.
137. **Kristo Väljako.** On the Morita equivalence of idempotent rings and monomorphisms of firm bimodules. Tartu, 2022, 139 p.
138. **Andre Ostrak.** Diameter two properties in spaces of Lipschitz functions. Tartu, 2022, 77 p.

139. **Mohammed Mainul Hossain.** Numerical analysis of vibrations of nano-beams. Tartu, 2022, 158 p.
140. **Alvin Lepik.** On Morita equivalence of semigroups. Tartu, 2023, 107 p.